21
150
R

KWAI S. CHAN
(210) 522-2053

Pages 1 Through 6 Are Intentionally
Left Blank

Jan 28, 1999

Work description: developed and finalized the work plan for rock fall modeling.

Performer: Dr. Kwai S. Chan

Rock Fall Modeling

The objective of this task is to develop a fracture mechanics-based model for treating the potential failure of degraded fuel cladding tubes caused by rock fall impacting on waste packages in the repository. The proposed approach is to treat degraded fuel cladding as internally pressured tubes containing surface or internal flaws. The size and shape of these flaws will be deduced from pertinent experimental data or information on the appropriate degradation mechanisms such as localized corrosion, hydride embrittlement, delayed hydride cracking, and fuel-side iodine-induced stress corrosion. Although these degradation processes may not lead to cladding failure under the nominal conditions anticipated in the repository, they can induce surface or internal cracks that may cause failure when the cladding are impacted by rock falls.

The rock fall model will be developed by treating the forces on the fuel cladding rods due to an impacting rock in terms of a distributed load. The fuel cladding is assumed to be degraded and contain cracks whose size and geometry are known. Based on these assumptions, the stresses in the cladding rods will be analyzed by performing the appropriate bending analysis and the relevant fracture mechanics parameters (stress intensity factor or the J-integral) will be obtained. The critical stress at the onset of cladding failure will be predicted based on a K_{IC} or J_{IC} criterion, depending on the amount of plastic flow associated with fracture. The critical stress will be predicted as a function of crack size including conditions where cracks are absent or small. Part of the proposed effect is to determine the possible size, shape, and orientation of cracks that might be present initially before emplacement or subsequently induced in the cladding by one or more of the pertinent degradation mechanisms after emplacement in the repository. Once the crack geometry is established, the failure of the fuel cladding subjected to impact loads resulting from rock fall will be modeled on the basis of linear-elastic fracture mechanics or elastic-plastic fracture mechanics. The proposed model will be used to assess the critical size and weight of rock fall required to cause cladding failure as a function of the angle, height and velocity of impacts, as well as the location, size, shape, and number of microcracks in the cladding.

Kwai S. Chan 1/28/99

Task 1. Rock Fall Modeling

Task 1.1. - Define flaw size, shape, and orientation.

Task 1.2 - Establish K and J-integral solutions for appropriate crack geometries

Task 1.3 - Interaction with PSU and Incorporation of impact load model.

Task 1.4 - Develop fracture mechanics model for predicting critical load and critical size of rock falls.

Task 1.5 - Exercise model to examine various rock fall scenarios.

Task 1.6 - Reporting.

Kwai S. Chan 1/28/99

Feb 2, 1999

Work Description: formulated an approach to treat fracture of Zr-cladding tubes for various crack sizes

Performer: Kwai S. Chan

Formulation of Fracture Approach

Approach: a fracture-mechanics-based approach that treats both small and large cracks in Zr-cladding tubes.

Assumptions:

1. A cladding tube containing a crack with length a is subject to an applied stress, σ.

2. Small-crack fracture in Zr-cladding can be treated in terms of the a_0 parameter that is defined as

$$a_0 = \frac{1}{\pi}\left[\frac{K_{IC}}{F\sigma_f}\right]^2$$

where K_{IC} is the critical stress intensity (fracture toughness) of the Zr-cladding tube, σ_f is the fracture strength or the ultimate fracture strength σ_{UTS}.

3. A K_{IC} fracture criterion holds for the Zr-cladding tubes. Both K_{IC} and σ_f are function of hydrogen content.

Kwai S. Chan 2/2/99

Fracture Modeling

The stress intensity factor, K, acting on the crack in the Zr-cladding tube is given by

$$K = F\sigma\sqrt{\pi(a+a_0)} \quad (1)$$

where F is the boundary correction factor, σ is the applied stress, and $a+a_0$ is the effective crack length that incorporates the small-crack effect.

The onset of fracture occurs when

$$K = K_{IC} \quad (2)$$

which leads to

$$F\sigma_{cr}\sqrt{\pi(a+a_0)} = K_{IC} \quad (3)$$

when (1) is set to (2) and $\sigma = \sigma_{cr}$ is invoked. Eq. (3) can be re-arranged to give

$$\sigma_{cr} = \frac{K_{IC}}{F\sqrt{\pi(a+a_0)}} \quad (4)$$

where σ_{cr} is the critical stress at fracture.

Fracture of smooth specimens of Zr-cladding occur at $\sigma_{cr} = \sigma_{UTS}$ and $a = 0$. Substituting these values into (4) gives

$$\sigma_{UTS} = \frac{K_{IC}}{F\sqrt{\pi a_0}} \quad (5)$$

Kwai S. Chan 2/2/99

leading to

$$a_0 = \frac{1}{\pi}\left[\frac{K_{IC}}{F\sigma_{UTS}}\right]^2 \quad (6)$$

Thus, the small-crack parameter a_0 can be calculated on the basis of K_{IC} and σ_{UTS}, both are material.

Substituting (6) into (4) leads one to

$$\sigma_{cr} = \frac{K_{IC}}{\sqrt{F^2\pi a + \left(\frac{K_{IC}}{\sigma_{UTS}}\right)^2}} \quad (7)$$

which reduces to

$$\sigma_{cr} = \sigma_{UTS} \quad \text{when} \quad a \to 0 \quad (8)$$

and

$$\sigma_{cr} = \frac{K_{IC}}{F\sqrt{\pi a}} \quad \text{when} \quad a \gg a_0 = \frac{1}{\pi}\left[\frac{K_{IC}}{F\sigma_{UTS}}\right]^2 \quad (9)$$

Thus, fracture of any crack size can be treated via Eq (3) or its equivalence, Eq (7).

Example: $K_{IC} = 20\ \mathrm{MPa}\sqrt{m}$
$\sigma_f = \sigma_{UTS} = 590$ MPa
$F = 1.12$ for edge crack

These values lead to the result shown in Figure 1, on the next page.

Kwai S. Chan 2/2/99

Filename : NRC-1.JNB
Date : 2/2/99

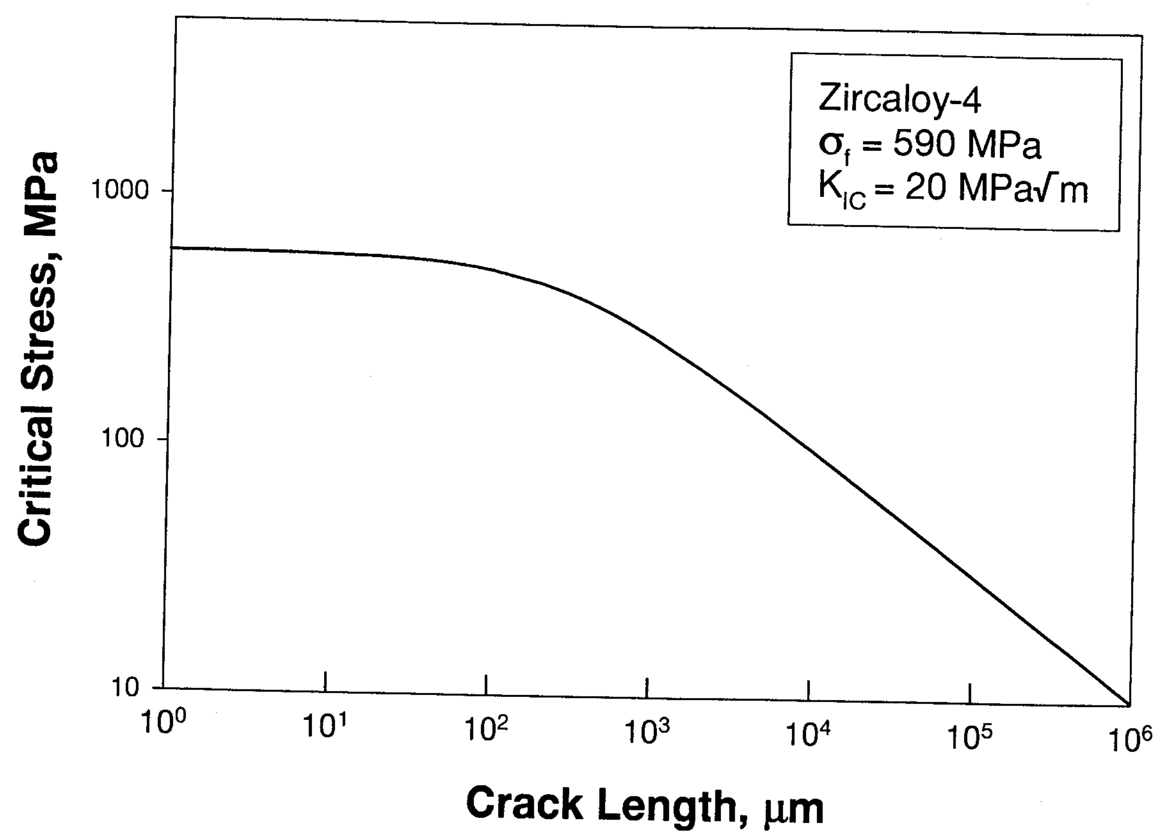

Kwai S. Chan 2/2/99

Feb 9, 1999

Work Description: calculate cladding stress due to rocks impacting on cladding tubes

Performer: Kwai S. Chan

Elastic Stress Analysis of a Cladding tube subjected to Rock Impact

Approach: treat the impact rock as a point load acting at the mid span of the cladding and apply bending theory to obtain the elastic stress on the cladding tube

Assumption: Spherical rock, solid tube; radius of rock = radius of rod

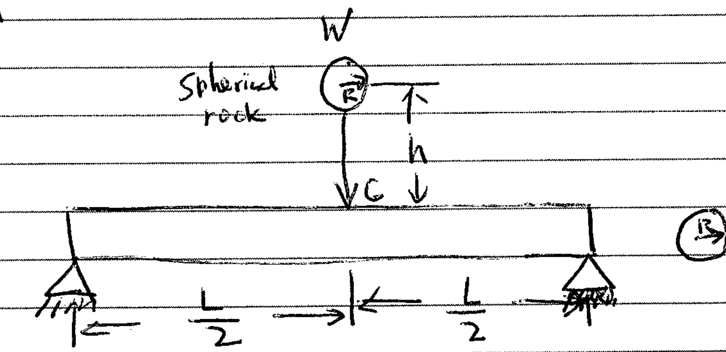

Nomenclature:

W : weight of rock
h : drop height
V : rock velocity
L : length of cladding rod
R : rod radius

References: Mechanics of Materials, by F.P. Beer and E. R. Johnston, Jr., McGraw-Hill, NY, 1981, pp. 497-498.

Kwai S. Chan 2/9/99

Objective: want cladding stress as a function of the drop height and ~~size~~ weight (K.C. 2/9/99) of rock

Solution: (from ref. 1)

Potential Energy (P.E.) = Wh

Kinetic Energy (K.E.) = $\frac{1}{2} mV^2$

Strain Energy (S.E) = $\frac{1}{2} P_m X_m$

where P_m is the maximum impact load or
X_m is the maximum deflection

An energy balance leads one to

$$Wh = \frac{1}{2} P_m X_m \qquad (1)$$

based on the assumption that the P.E. of the rock goes to deform the rod elastically

From beam deflection theory (Ref. 1, p. 497 and 598), one obtain

$$X_m = \frac{P_m L^3}{48 E I} \qquad (2)$$

with $I =$ ~~[illegible]~~ (K.C. 2/9/99) $= \frac{\pi}{4} R^4$ for ~~[illegible]~~ solid tube (K.C. 2/9/99)

Equating (1) to (2) leads one to

$$Wh = \frac{1}{2} P_m \left(\frac{P_m L^3}{48 E I} \right)$$

Kevin S. Chan 2/9/99

leading to

$$P_m = \left[\frac{96 E I W h}{L^3} \right]^{1/2} \qquad (3)$$

From bending theory, the maximum stress, σ_m, at C is given by

$$\sigma_m = \frac{M_{ax} C}{I} = \frac{M_{ax} R}{I} = \frac{P_m L R}{4 I} \qquad (4)$$

Substituting (3) into (4) gives

$$\sigma_m = \left[\frac{96 E I W h}{L^3} \right]^{1/2} \left[\frac{L R}{4 I} \right]$$

$$\Rightarrow \sigma_m = \left[\frac{6 E W h R^2}{L I} \right]^{1/2} \qquad (5)$$

Combining (5) with

$$I = \frac{\pi}{4} R^4 \qquad (6)$$

and

$$W = \rho V = \frac{4}{3} \pi R^3 \rho g \qquad (7)$$

where ρ is the rock density, gives

$$\sigma_m = \left[\frac{6 E \rho g \cdot \frac{4}{3} \pi R^3 \cdot h R^2}{L \cdot \frac{\pi}{4} R^4} \right]^{1/2}$$

$$\Rightarrow \sigma_m = \left[\frac{96 E \rho g R h}{3 L} \right]^{1/2} \qquad (8)$$

Kevin S. Chan 2/9/99

E of Zircaloy = 9.9284×10^4 MPa
R of Zircaloy Rod = 5×10^{-3} m
h = 0.2 m
L = 15 in = 0.381 m
ρ = 2297 kg/m³; $\rho g = 2.252 \times 10^4$ N/m³

$$\sigma_m = \left[\frac{96 \times 9.9284 \times 10^{10}\ N/m^2 \times 2.252 \times 10^4\ N/m^2 \times 5 \times 10^{-3}\ m\ h}{3(0.381\ m)}\right]^{1/2}$$

$$\sigma_m = 30.6423\ h^{1/2}\ \text{MPa} \quad (h \text{ in } m)$$

σ_{ys} of Zircaloy = 801 MPa

Filename: Rock-1.jnb

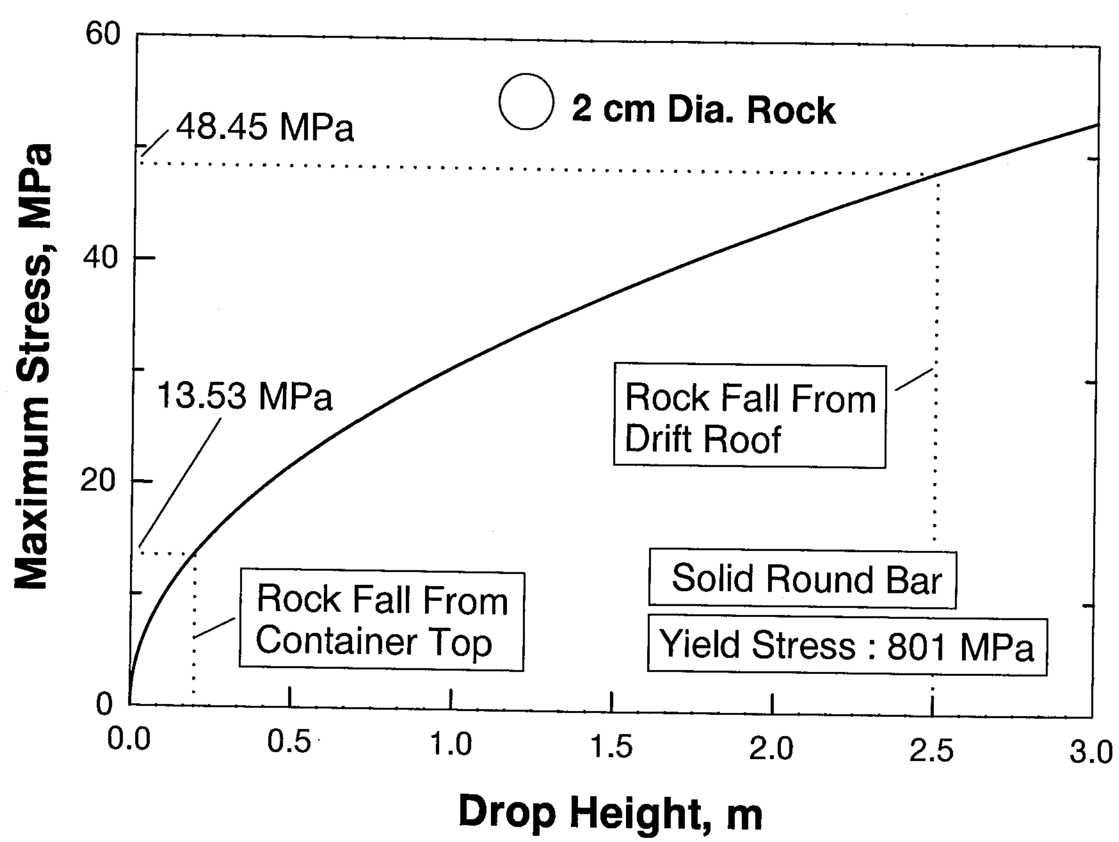

Finding: small rock impact induces a very low stress on the cladding tube.

Kwai S. Chan 2/9/99

Feb 15, 1999

Cylindrical Rock: impacting on solid tube

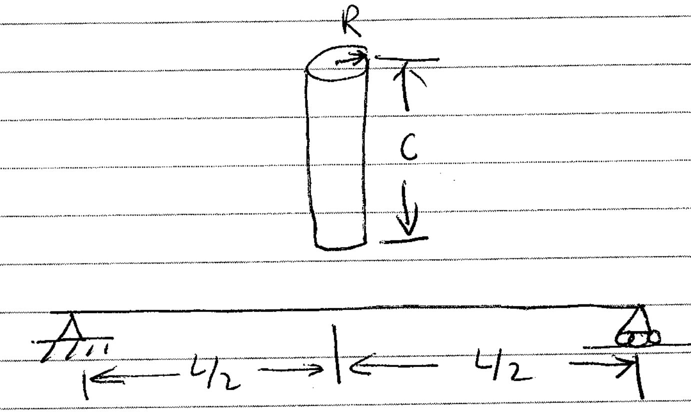

From Eq ⑤

$$\sigma_m = \left[\frac{6EWhR^2}{LI}\right]^{1/2}$$

For cylindrical rock

$W = \rho \pi R^2 c g$ where ρ is rock density, g is gravity

$I = \frac{1}{4}\pi R^4$

Then
$$\sigma_m = \left[\frac{6E\rho\pi R^2 c h R^2 g}{L \cdot \frac{1}{4}\pi R^4}\right]^{1/2}$$

$$\Rightarrow \quad \sigma_m = \left[\frac{24E\rho c h g}{L}\right]^{1/2} \qquad (9)$$

Kwai S. Chan

2/15/99

For $h = 0.2$ m $E = 9.9284 \times 10^4$ MPa

$\rho g = 2.254 \times 10^4$ N/m^2

$L = 0.381$ m

$\sigma_m = 1.67835 \times 10^2 \, c^{1/2}$ MPa (c in m)

Filename: Rock-1.jnb

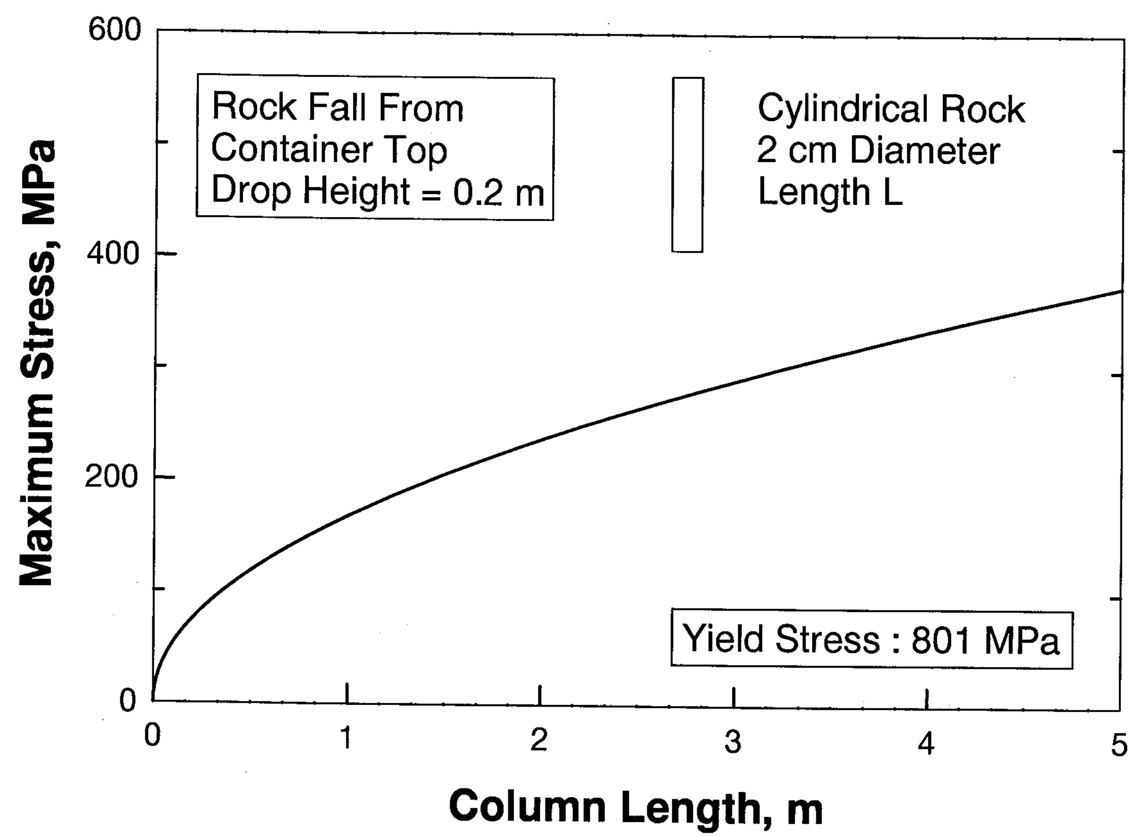

Kwai S. Chan 2/15/99

For $h = 2.5$ m

$E = 9.9284 \times 10^4$ MPa

$\rho g = 2.254 \times 10^4$ N/m^2

$L = 0.381$

$\sigma_m = 5.93386 \, c^{1/2}$ MPa (c in m)

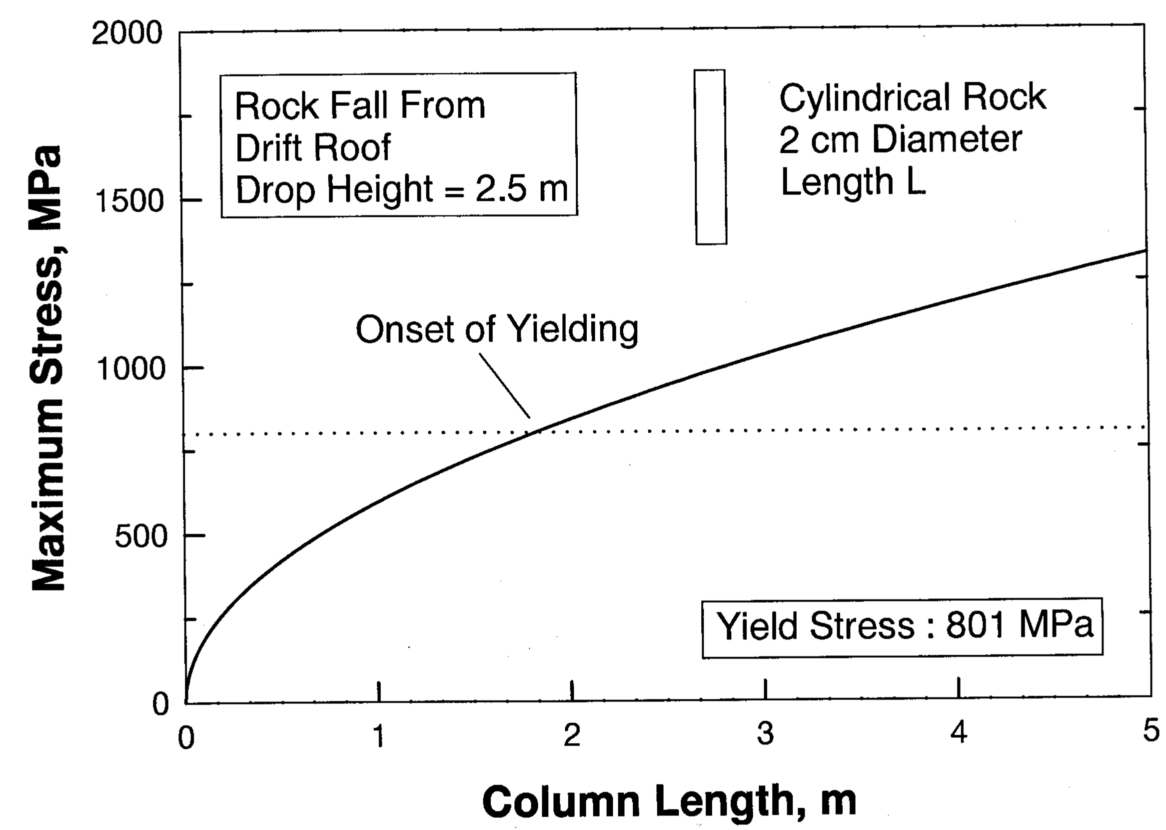

Kwai S. Chan 2/15/99

Feb 22, 1999

Disk-Like Rock

K.C. 2/22/99

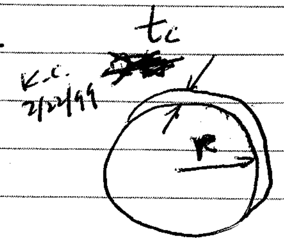

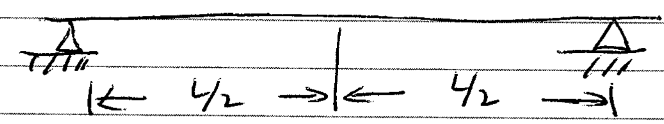

where t_c = thickness of rock ≈ R

r = rock radius

K.C. 2/22/99 assume $t_c = R$

From Eq (5)

$$\sigma_m = \left[\frac{6EWhR^2}{LI}\right]^{1/2}$$

For disk-like rock

K.C. 2/22/99

$$W = \rho R \pi r^2 g$$

$$I = \frac{1}{4}\pi R^2$$

K.C. 2/22/99

then
$$\sigma_m = \left[\frac{6E(R\rho\pi r^2 g)h}{L\cdot\frac{1}{4}\pi R^2}\right]^{1/2}$$

$$\sigma_m = \left[\frac{24E\rho r^2 gh}{LR}\right]^{1/2} \quad (10)$$

Filename = Rock-1.jnb

dropheight = 0.2 m and 2.5 m

Kwai S. Chan 2/22/99

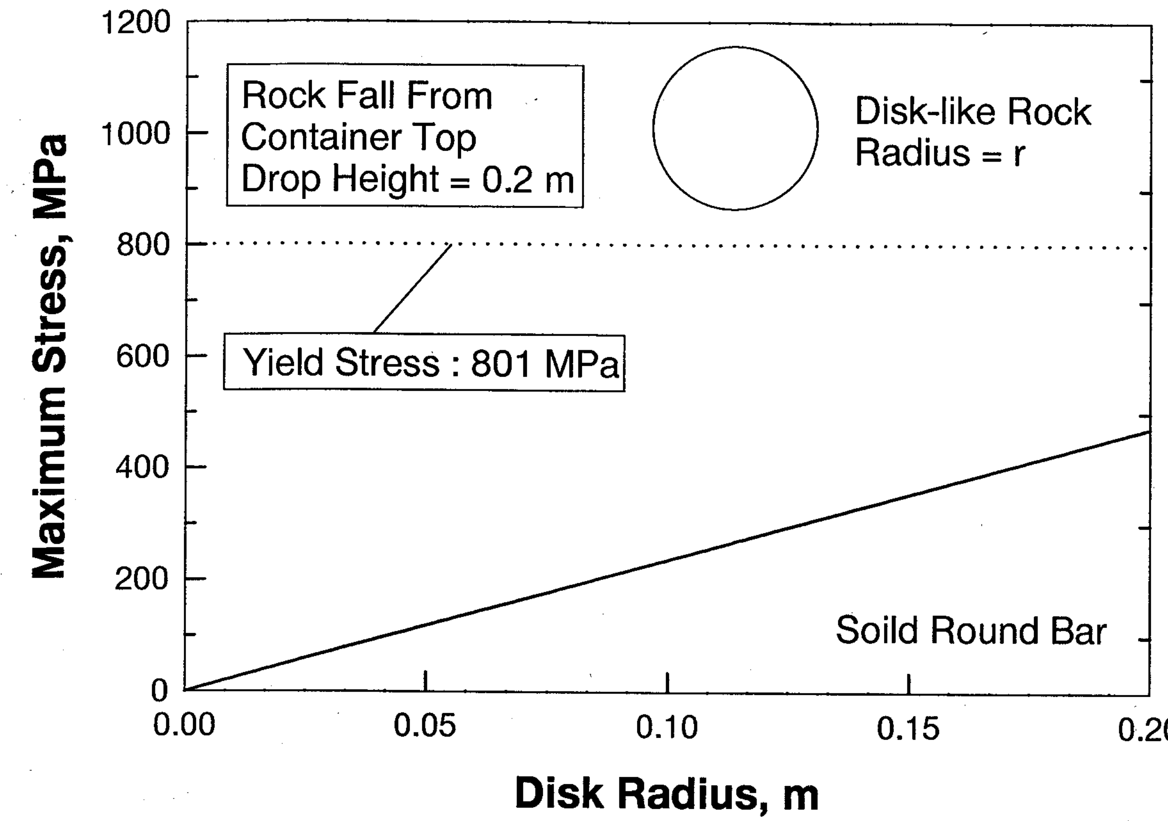

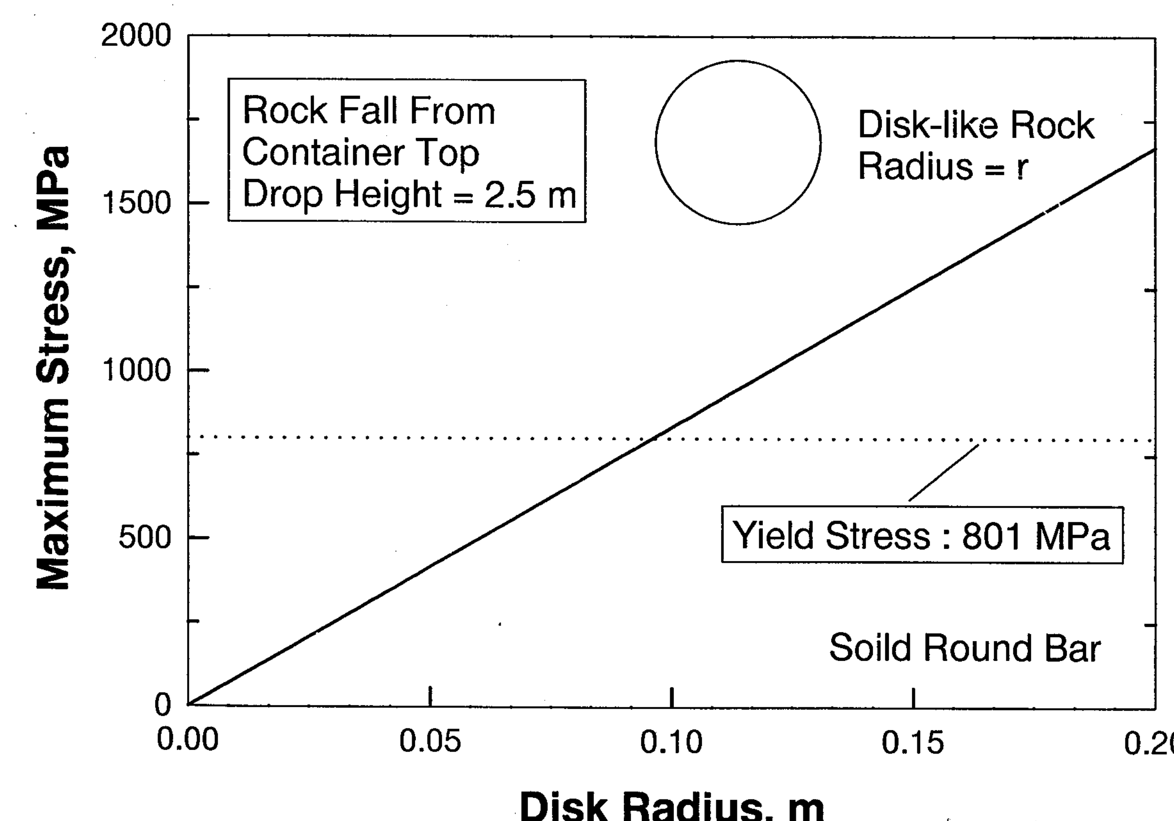

Kwai S. Chan 2/22/99

March 1, 1999

Spherical Rocks / Thin-Walled Tubes

From Eq (3) $\quad P_m = \left[\dfrac{96EIWh}{L^3}\right]^{1/2}$

For thin-walled tubes

$$I = \frac{1}{4}\pi\left(r_o^4 - r_i^4\right)$$

$$= \frac{1}{4}\pi r_o^4\left[1 - \left(\frac{r_i}{r_o}\right)^4\right]$$

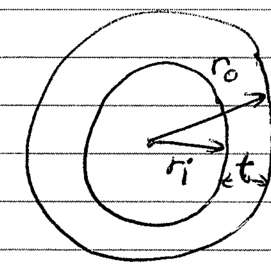

Let $r_o = R$ and $r_i = R - t$

Then

$$I = \frac{1}{4}\pi R^4\left[1 - \left(\frac{R-t}{R}\right)^4\right] \qquad (11)$$

From Eq (5)

$$\sigma_m = \left[\frac{6EWhR^2}{LI}\right]^{1/2}$$

and $I = \frac{1}{4}\pi R^4\left[1 - \left(\frac{R-t}{R}\right)^4\right]$

$$\Rightarrow \sigma_m = \left[\frac{6EWhR^2}{L\cdot\frac{1}{4}\pi R^4\cdot\beta}\right]^{1/2}$$

Where $\beta = 1 - \left(\dfrac{R-t}{R}\right)^t$ (11a)

leading to $\sigma_m = \left[\dfrac{1}{\beta}\right]^{1/2}\left[\dfrac{24EWh}{\pi R^2 L}\right]^{1/2}$

Kwai S. Chan 3/1/99

Since $W = \rho\left(\frac{4}{3}\pi R^3\right)g$

By substitution W into σ_m equation, then

$$\sigma_m = \left[\frac{1}{\beta}\right]^{1/2}\left[\frac{24E\rho\cdot\frac{4}{3}\pi R^3 hg}{\pi R^2 L}\right]^{1/2}$$

$$\sigma_m = \left[\frac{1}{\beta}\right]^{1/2}\left[\frac{96E\rho hg}{3L}\right]^{1/2}$$

↑ correction for thin-walled tubes

← solid rod solution

$r_o = 0.391$ in$/2$
$r_i = 0.367$ in$/2$

$R = \dfrac{r_i + R_o}{~~4~~ 2} = \dfrac{0.379 \text{ in}}{2} = 0.1895$ in

$$\left[\sigma_m\right]_{\text{thin-walled tube}} = \left[\frac{1}{1-\left(\frac{r_i}{r_o}\right)^4}\right]^{1/2}\left[\sigma_m\right]_{\text{solid bar}} \qquad (12)$$

$$\left[\sigma_m\right]_{\text{thin-walled tube}} = \left[\frac{1}{1-\left(\frac{0.367}{0.391}\right)^4}\right]^{1/2}\left[\sigma_m\right]_{\text{solid bar}} \qquad ~~(13)~~$$

K.C. 3/1/99

$$\left[\sigma_m\right]_{\text{thin-walled tube}} = 2.11369\left[\sigma_m\right]_{\text{solid bar}}$$

Kwai S. Chan 3/1/99

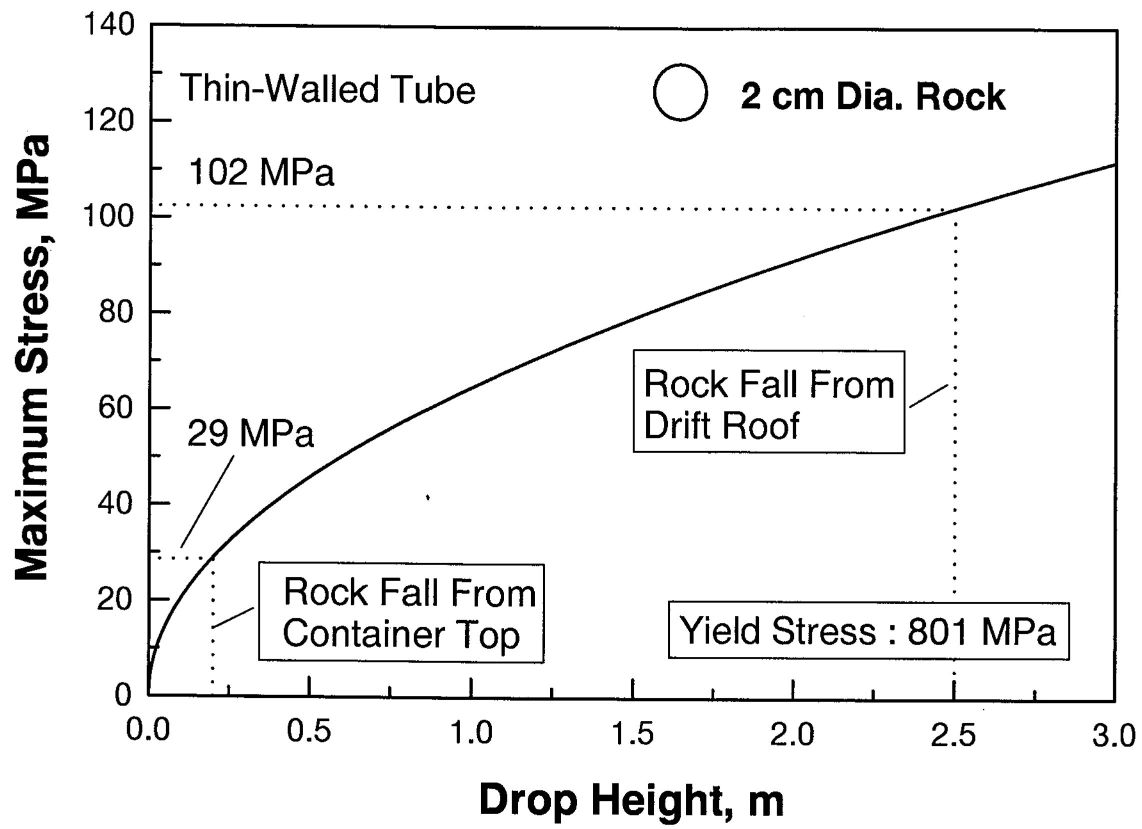

Kwai S. Chan 3/1/99

3/3/99

Thin-Walled Tubes/Cylindrical Rock:

From Eq 6. $\sigma_m = \left[\dfrac{6 E w h R^2}{L I}\right]^{1/2}$

For cylindrical rock: $W = \rho \pi R^2 c g$

$$I = \frac{1}{4}\pi R^4 \left[1 - \left(\frac{R-t}{R}\right)^4\right] = \frac{1}{4}\pi R^4 \beta$$

$$\sigma_m = \left[\frac{6 E \rho \pi R^2 c h R^2 g}{L \cdot \frac{1}{4}\pi R^4 \cdot \beta}\right]^{1/2}$$

$$= \left[\frac{1}{\beta}\right]^{1/2} \left[\frac{24 E \rho g c h}{L}\right]^{1/2}$$

$$[\sigma_m]_{\text{thin-walled tube}} = \left[\frac{1}{\beta}\right]^{1/2} [\sigma_m]_{\text{solid bar}}$$

$$[\sigma_m]_{\text{thin-walled tubes}} = 2.11369\, [\sigma_m]_{\text{solid bar}} \qquad (14)$$

3/3/99 Kwai S. Chan

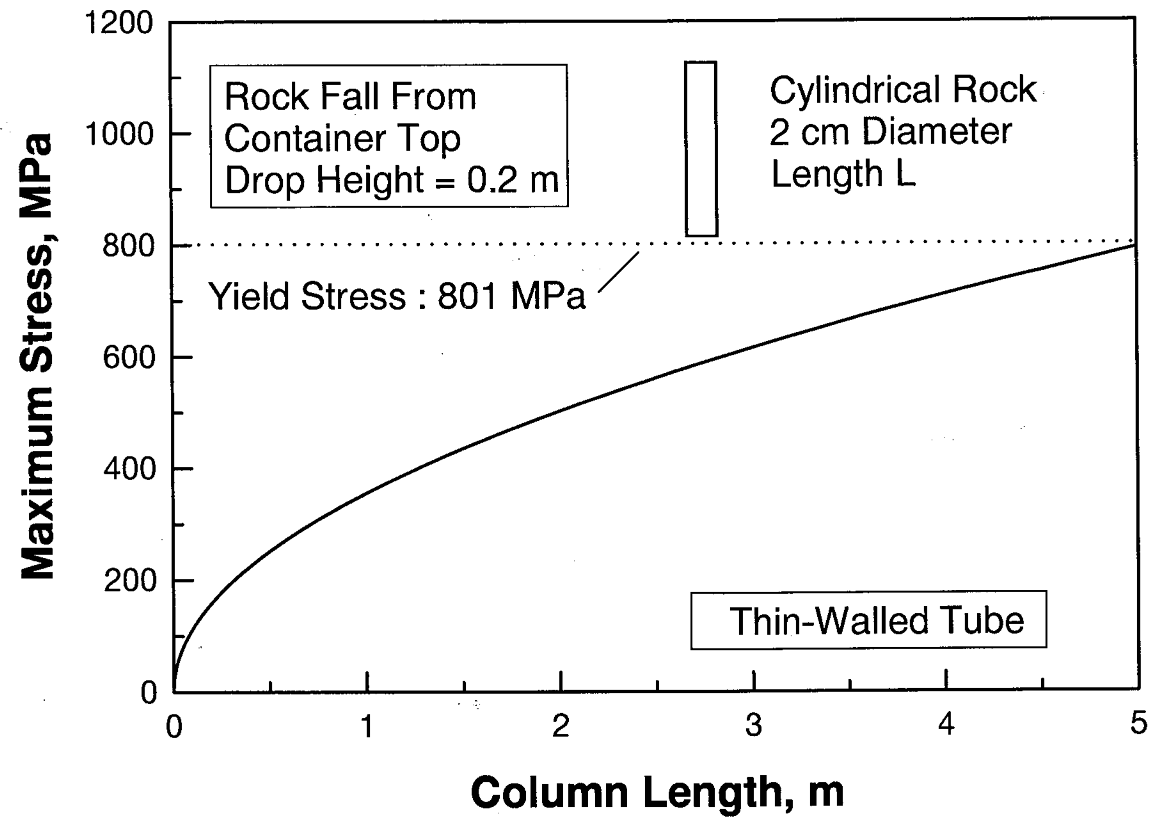

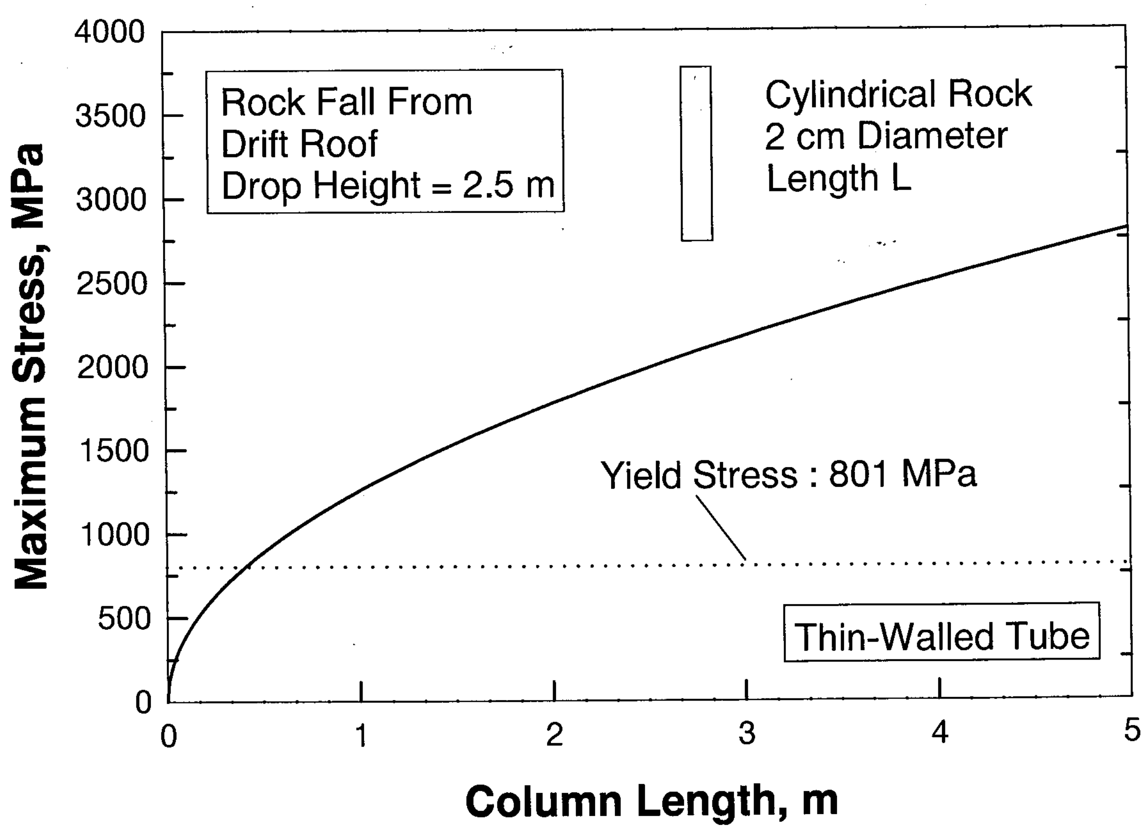

Kwai S. Chan 3/3/99

3/11/99

Disk-Like Rock / Thin-Walled Tubes

From Eq (5)

$$\sigma_m = \left(\frac{6 E W h R^2}{L I} \right)^{1/2}$$

Since $W = \rho \pi r^2 R g$

$I = \frac{1}{4} \pi R^4 \beta$ $\quad \beta$ given by Eq. (11a)

Then

$$[\sigma_m]_{\text{thin-walled tube}} = \left[\frac{6 E \rho R r^2 \pi R^2 g}{L \cdot \frac{1}{4} \pi R^4 \beta} \right]^{1/2}$$

$$[\sigma_m]_{\text{thin-walled tube}} = \left[\frac{1}{\beta} \right]^{1/2} \left[\frac{24 E \rho g r^2}{L R} \right]^{1/2}$$

$$[\sigma_m]_{\text{thin-walled tube}} = \left[\frac{1}{\beta} \right]^{1/2} [\sigma_m]_{\text{solid bar}} \qquad (15)$$

Kwai S. Chan 3/11/99

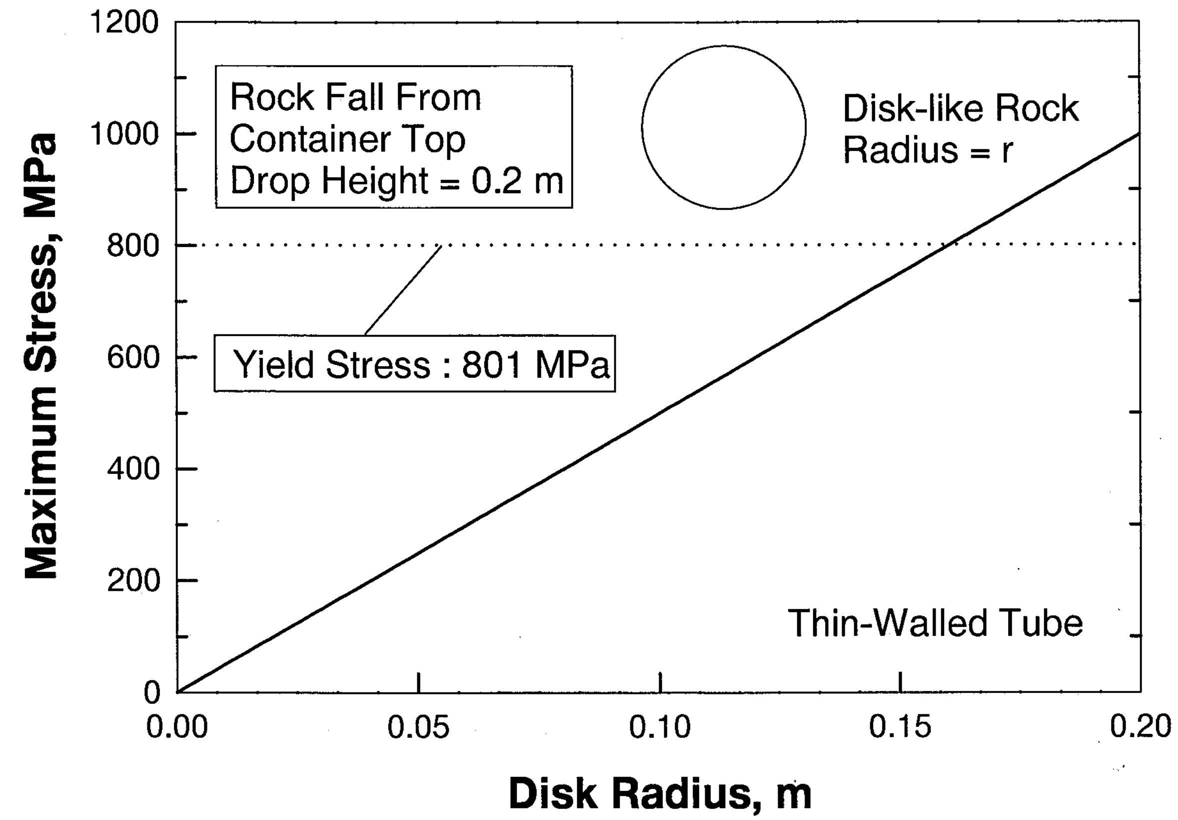

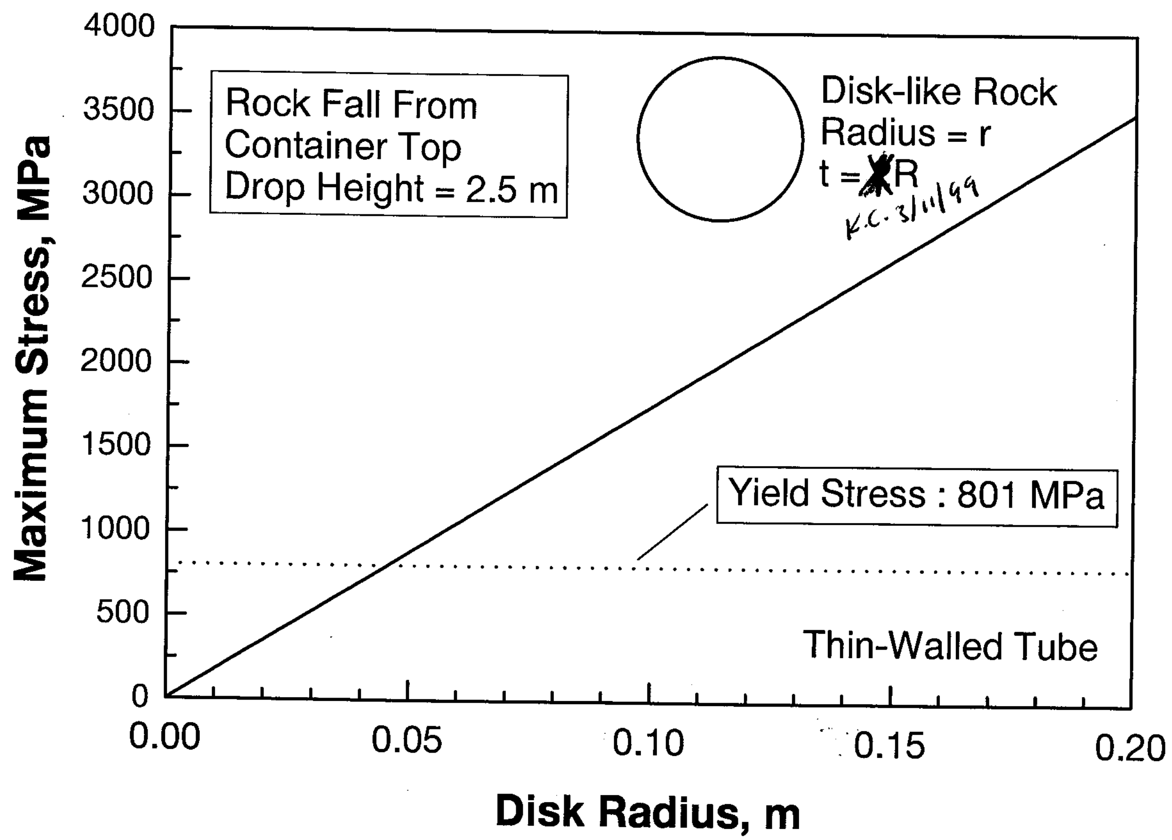

Kwai S. Chan 3/11/99

March 12, 1999

Reviewed K solutions of thin-walled tubes subjected to axial loading and bending

Selected the K solutions obtained by Bergman (1995). (Fat. Fract. Eng. Mat. Struct., 18, 1995, pp. 1155–1172).

$$K_I = f_i \sigma_i \sqrt{\pi a} \quad (16)$$

where K_I = mode I stress intensity factor

σ_i = stress on the mode I crack

a = crack depth of a ~~[illegible]~~ surface crack with length ~~[illegible]~~ 2c and depth a (see Figure for crack geometry). K.C. 3/12/99

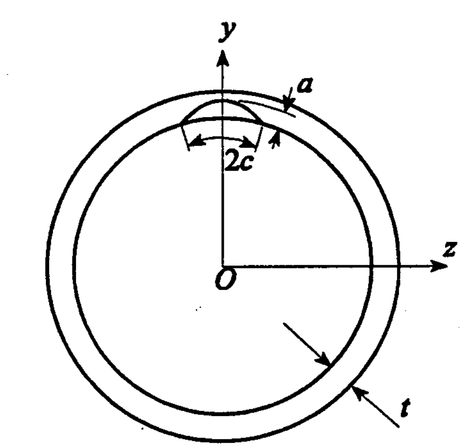

Circumferential inside surface crack in a cladding. K solutions are given in the paper by Bergman (1995).

Kwai S. Chan 3/12/99

Six different load cases were considered by Bergman, who gave

$$\sigma = \sigma_0 + \sigma_1\left(\frac{u}{a}\right) + \sigma_2\left(\frac{u}{a}\right)^2 + \sigma_3\left(\frac{u}{a}\right) + \sigma_4(Y/R_o) + \sigma_5(Z/R_o) \quad (17)$$

KC. 3/12/99

where u is a local ~~...~~ normalized radial coordinate from the tube surface to the full crack depth a.

Ro is the outside radius

The geometry correction factor f_i is given by (Bergman, 1995)

$$f_i = A_0 + A_1\left(\frac{2\phi}{\pi}\right) + A_2\left(\frac{2\phi}{\pi}\right)^2 + A_3\left(\frac{2\phi}{\pi}\right)^3 + A_4\left(\frac{2\phi}{\pi}\right)^4 + A_5\left(\frac{2\phi}{\pi}\right)^5 + A_6\left(\frac{2\phi}{\pi}\right)^6 \quad (18)$$

ϕ is the angular position of the crack front measured from the crack surface

$\phi = 0$ at the crack surface

$\phi = 90°$ at the crack depth.

A_i is a function of a/t as given by

$$A_i = b_{0,i} + b_{1,i}(a/t) + b_{2,i}(a/t)^2 \quad (19)$$

where $b_{0,i}$, $b_{1,i}$, and $b_{2,i}$ are tabulated constants ~~from Bergman (1995)~~ obtained by fitting Ao as a function of a/t

KC. 3/12/99

Kwai S. Chan 3/12/99

3/15/99

The regression analyses were performed using values of Ai reported by Bergman (1995). These analyses were performed for various loading types (σ_4, σ_5 etc) and various c/a ratios (1, 2, 4, 8, 16) and R/t ratio (=10).

Results for σ_4 type loading, R/t = 10 and c/a = 1 are shown next. σ_4-type loading is bending.

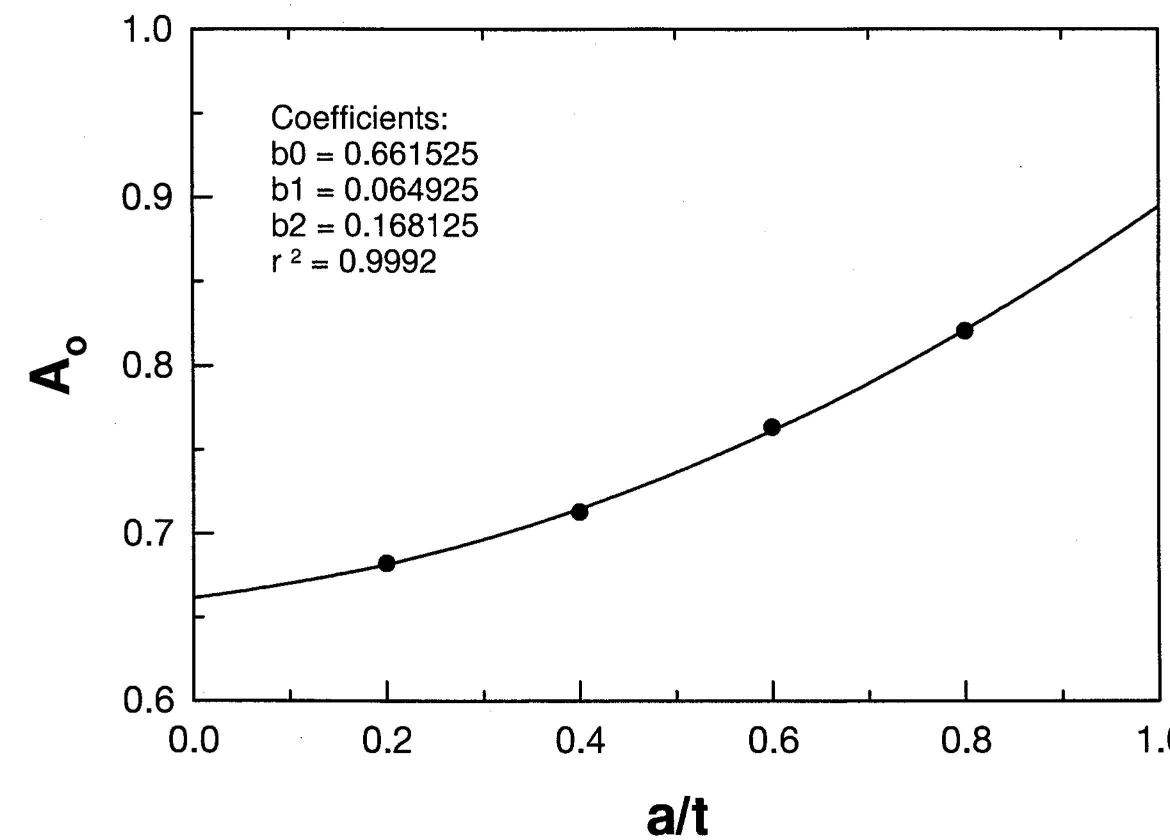

Kwai S. Chan 3/15/99

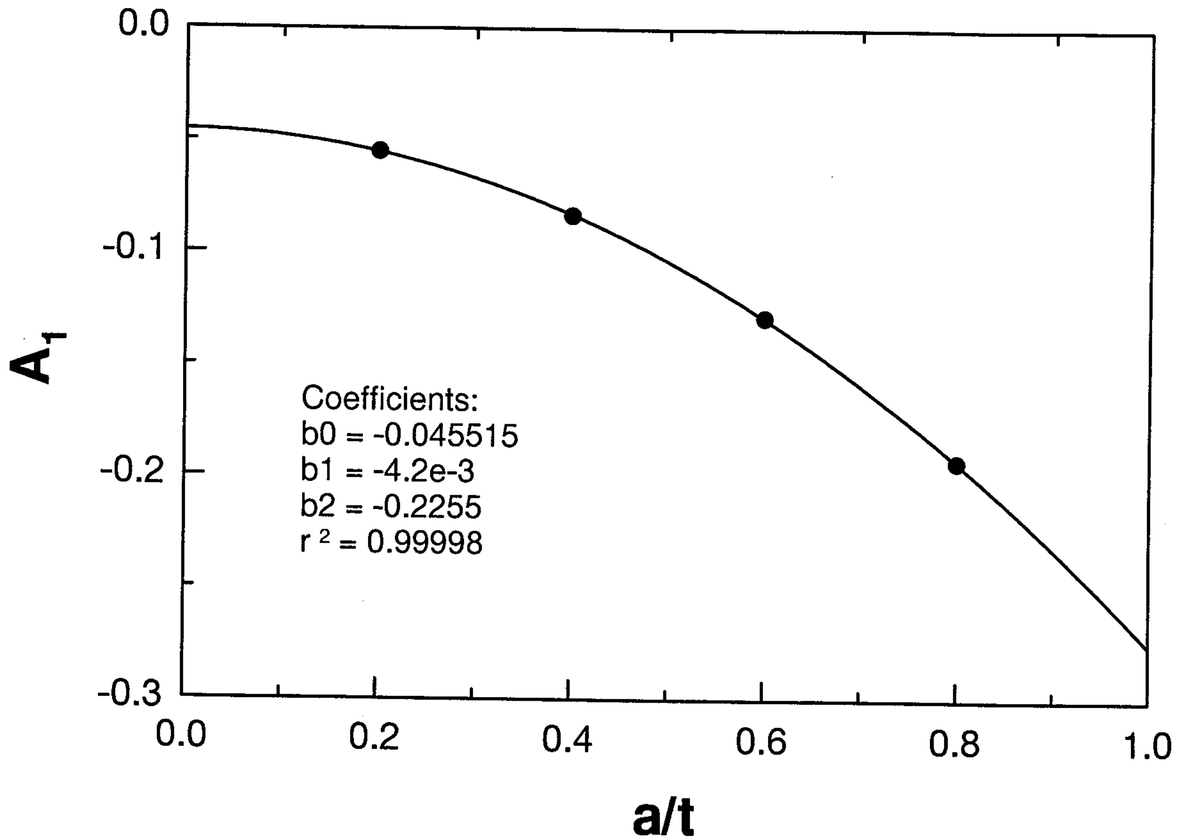

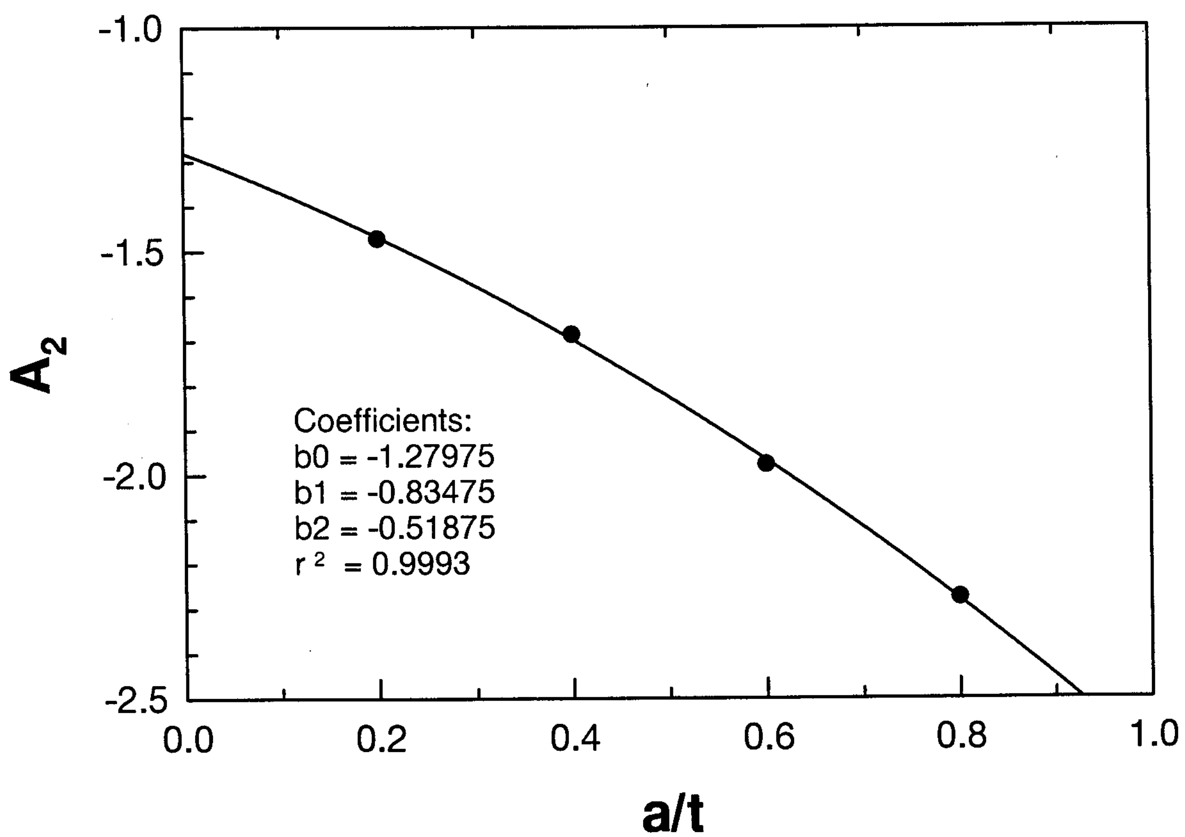

Kwai S. Chan 3/15/99

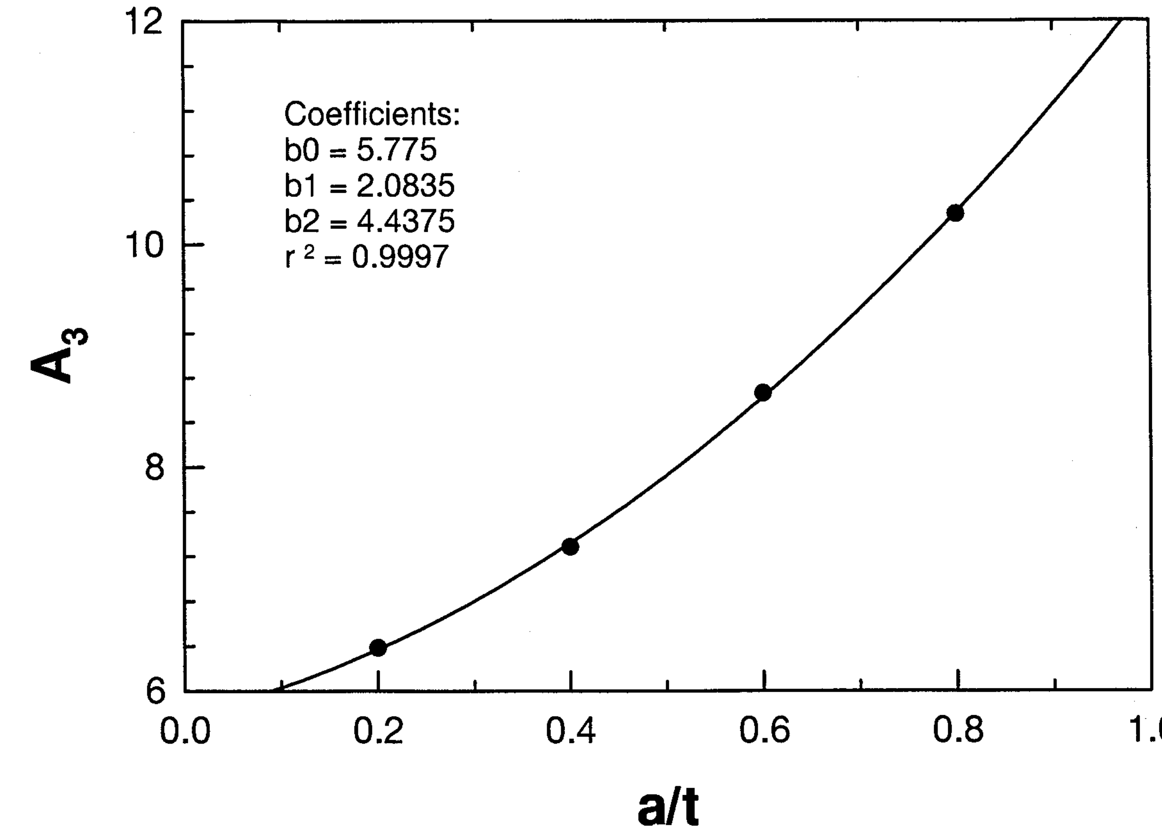

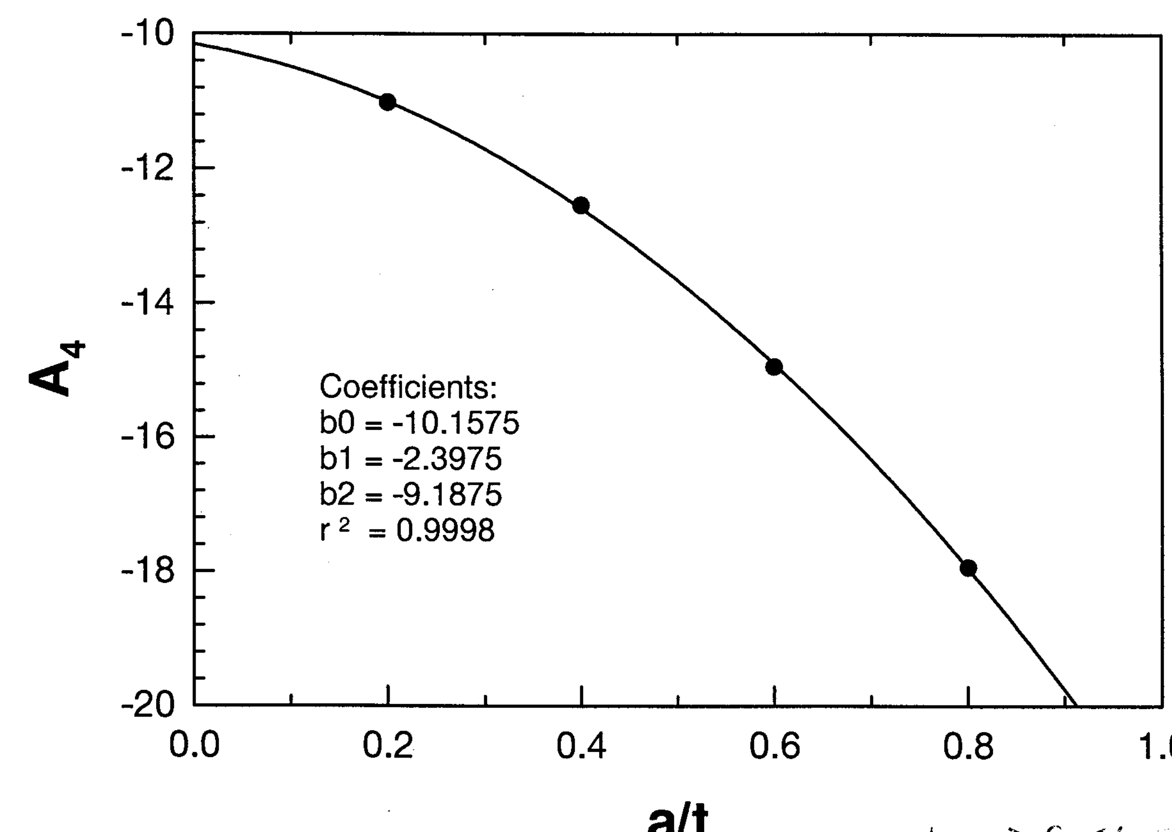

Kwai S. Chan 3/15/99

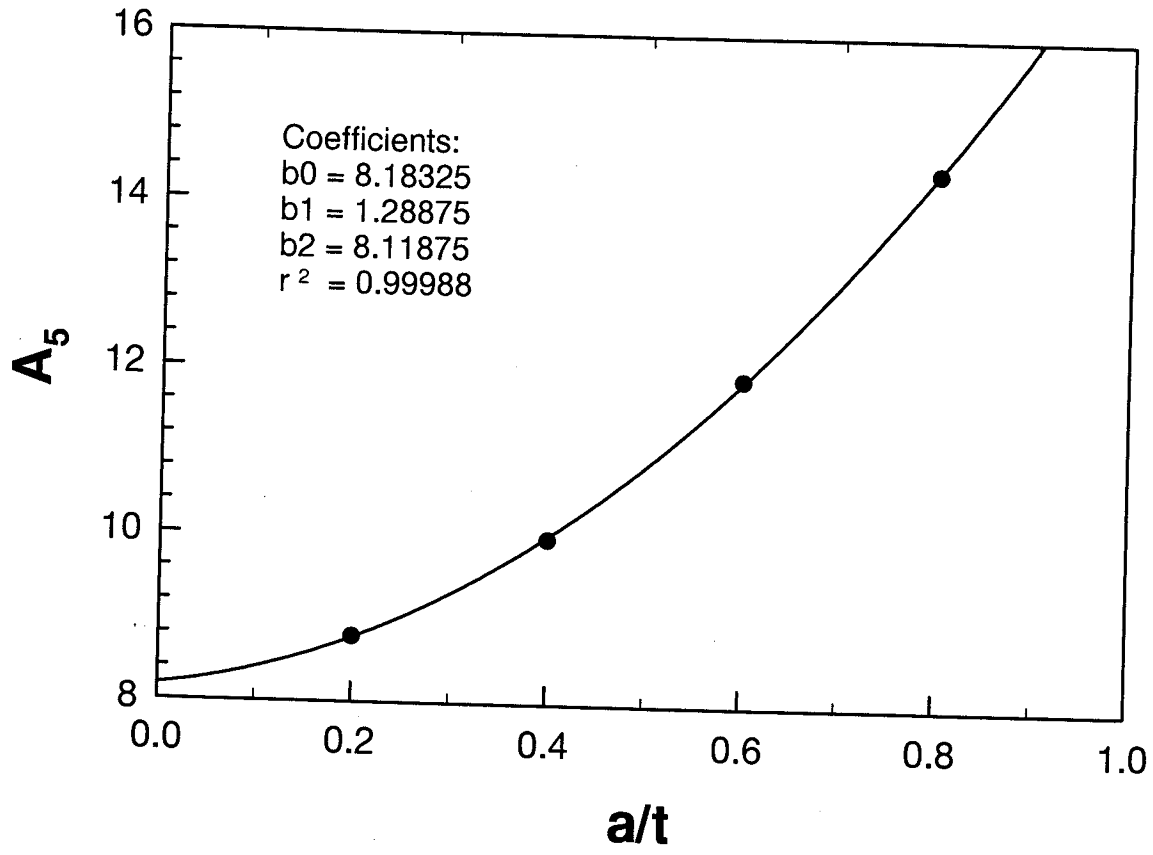

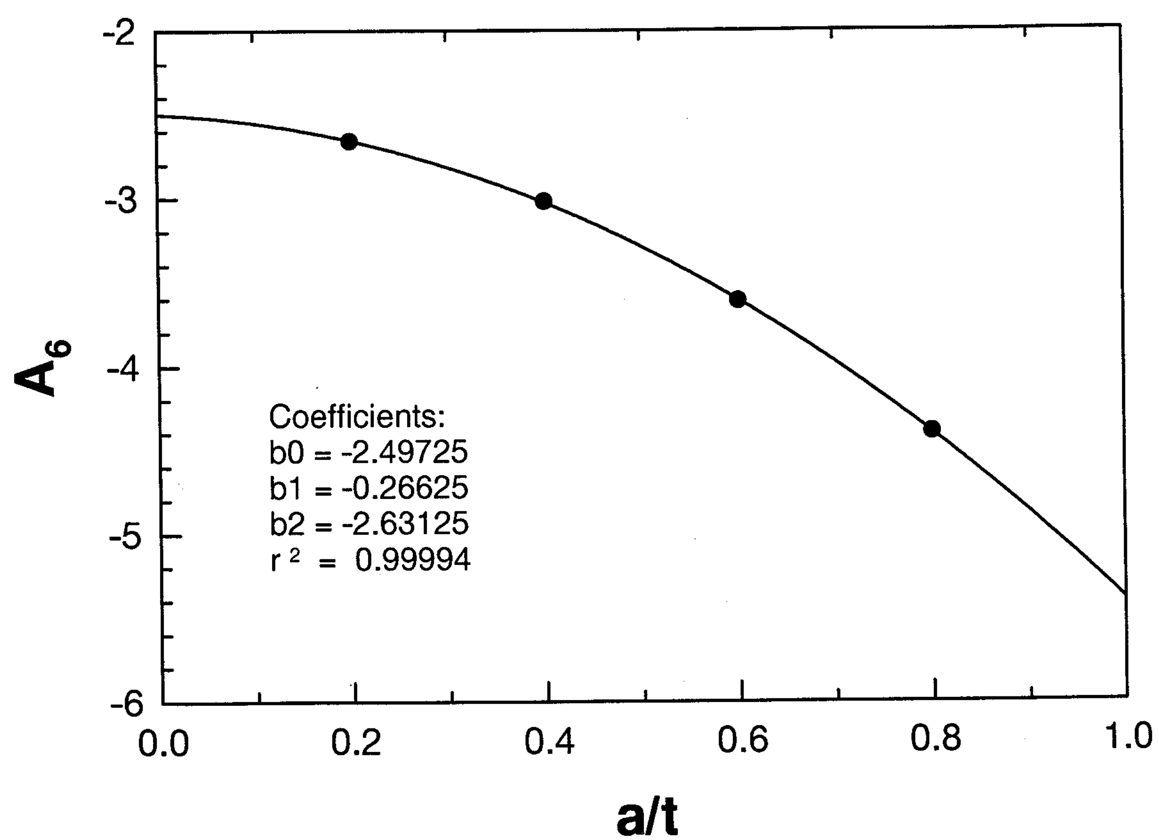

Kwai S. Chan 3/15/99

3/26/99

σ5 loading R/t = 10 c/a = 1

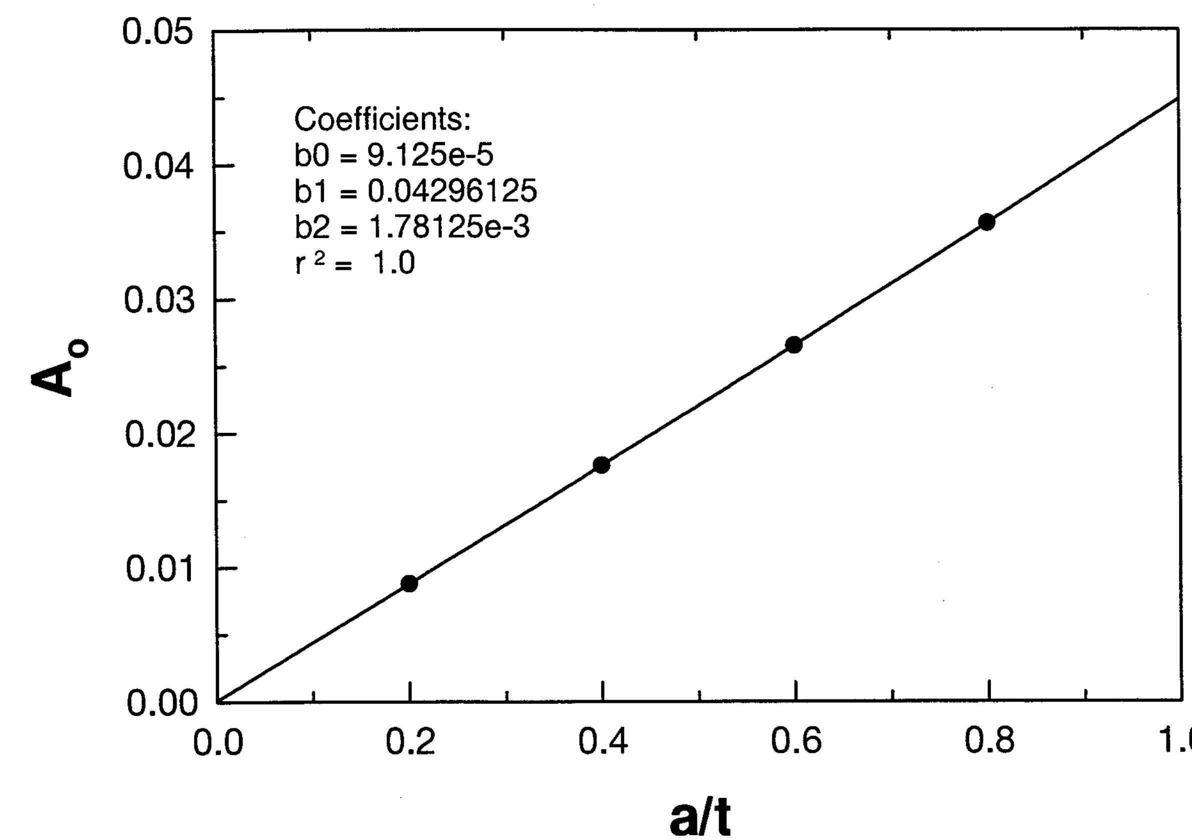

Kwai S. Chan 3/26/99

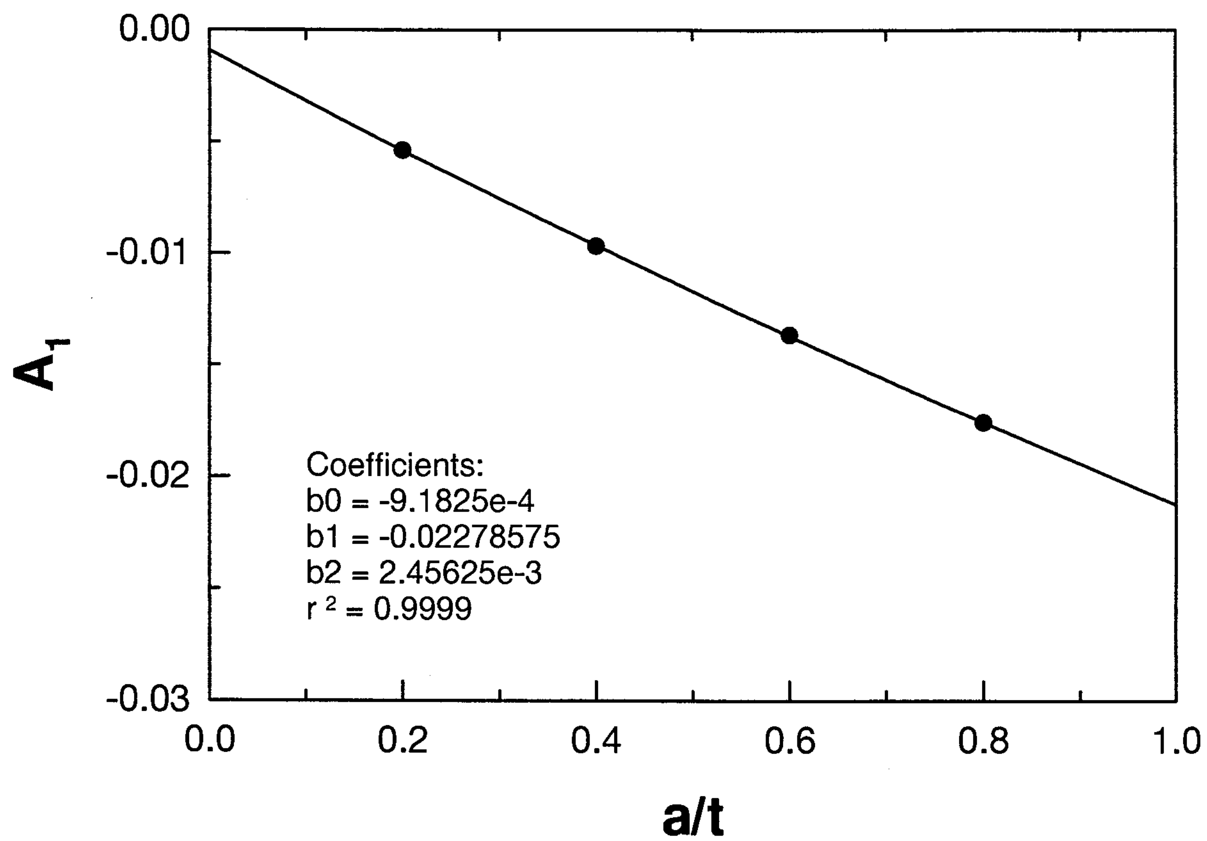

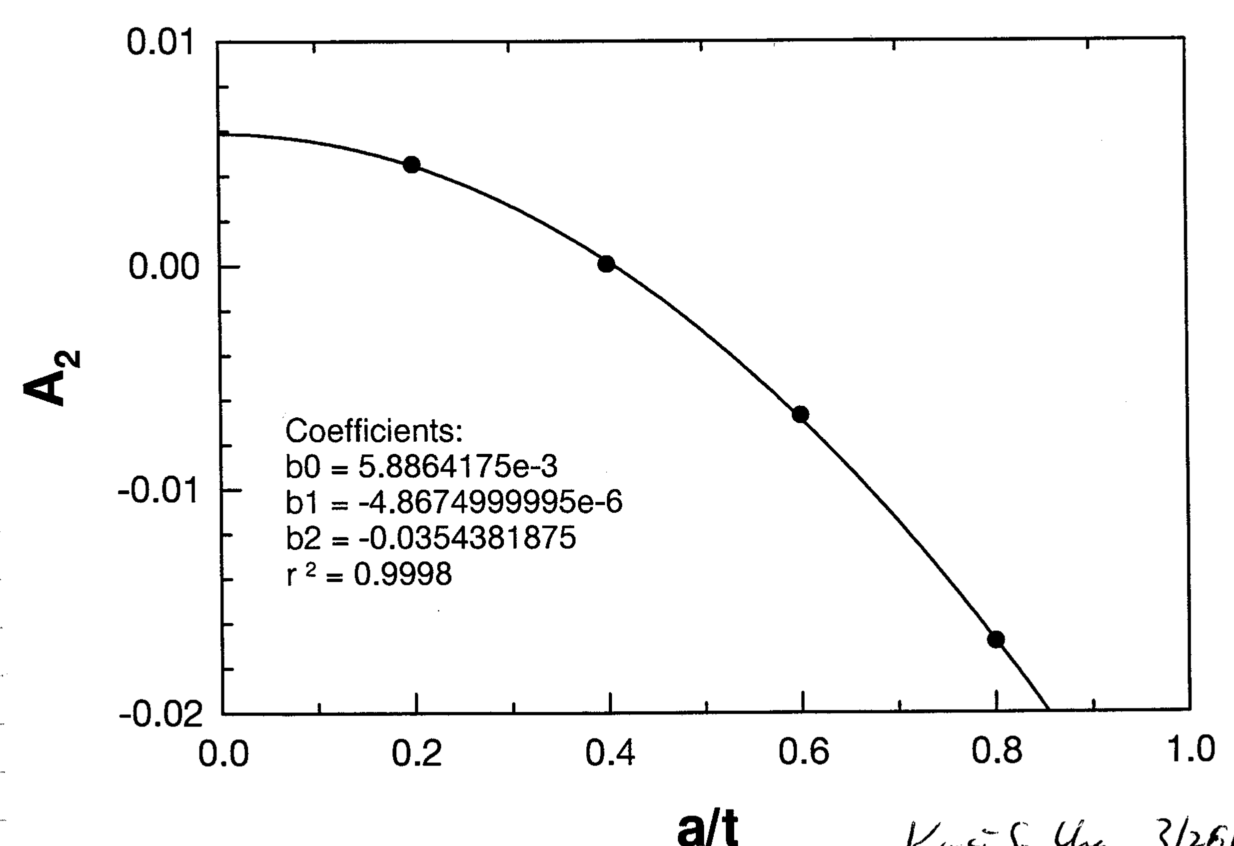

Kwai S. Chan 3/26/99

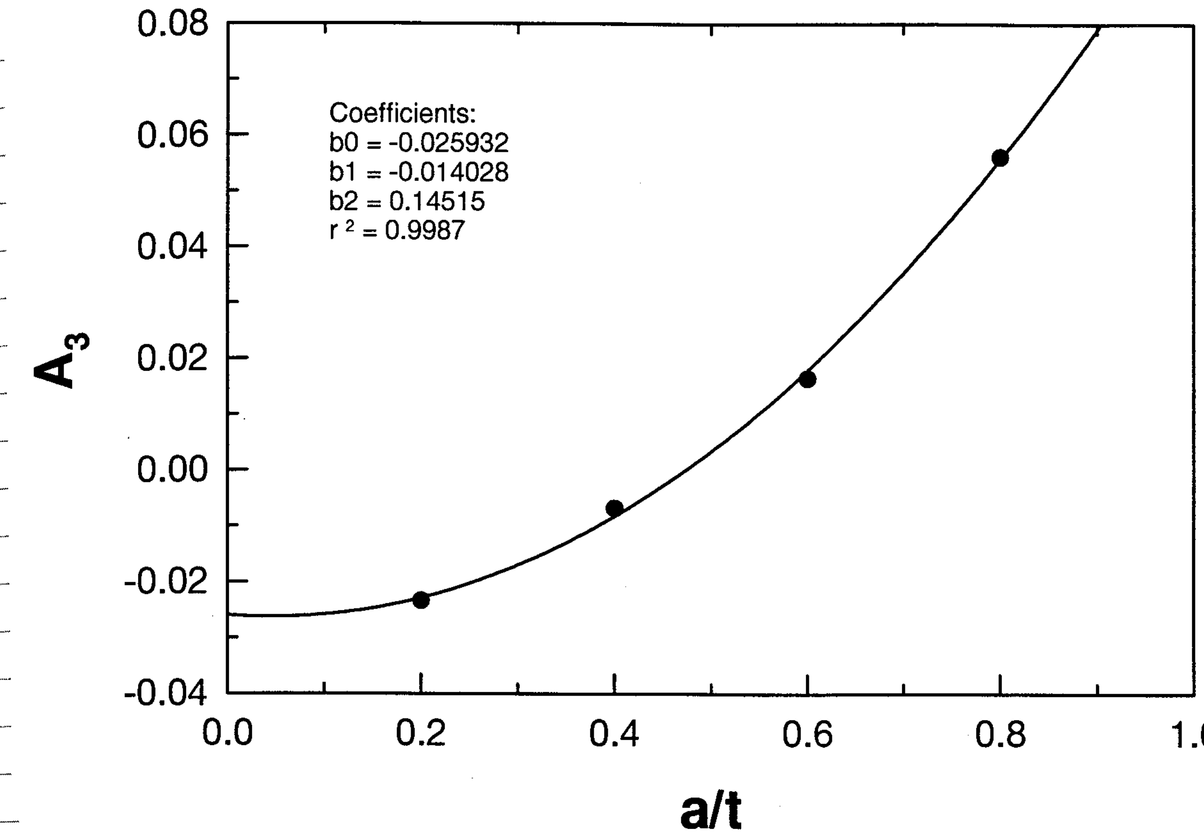

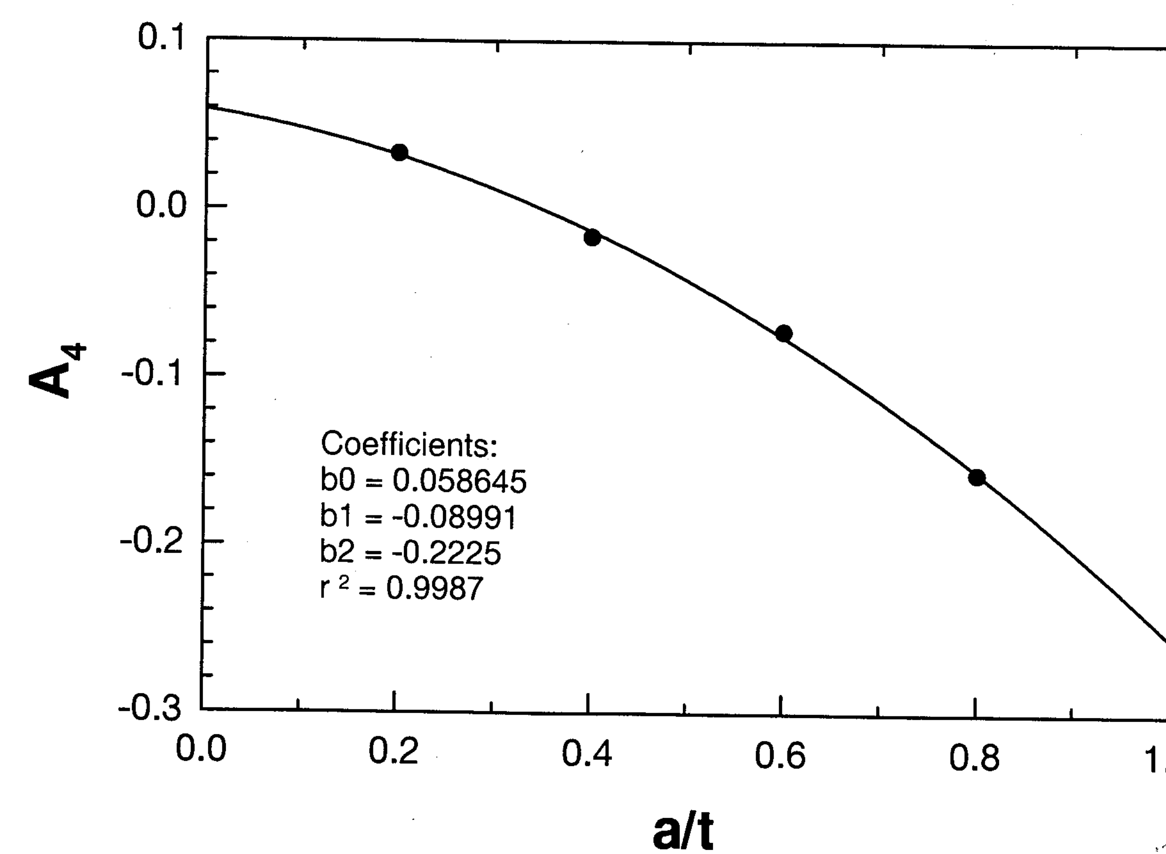

Kwai S. Chan 3/26/99

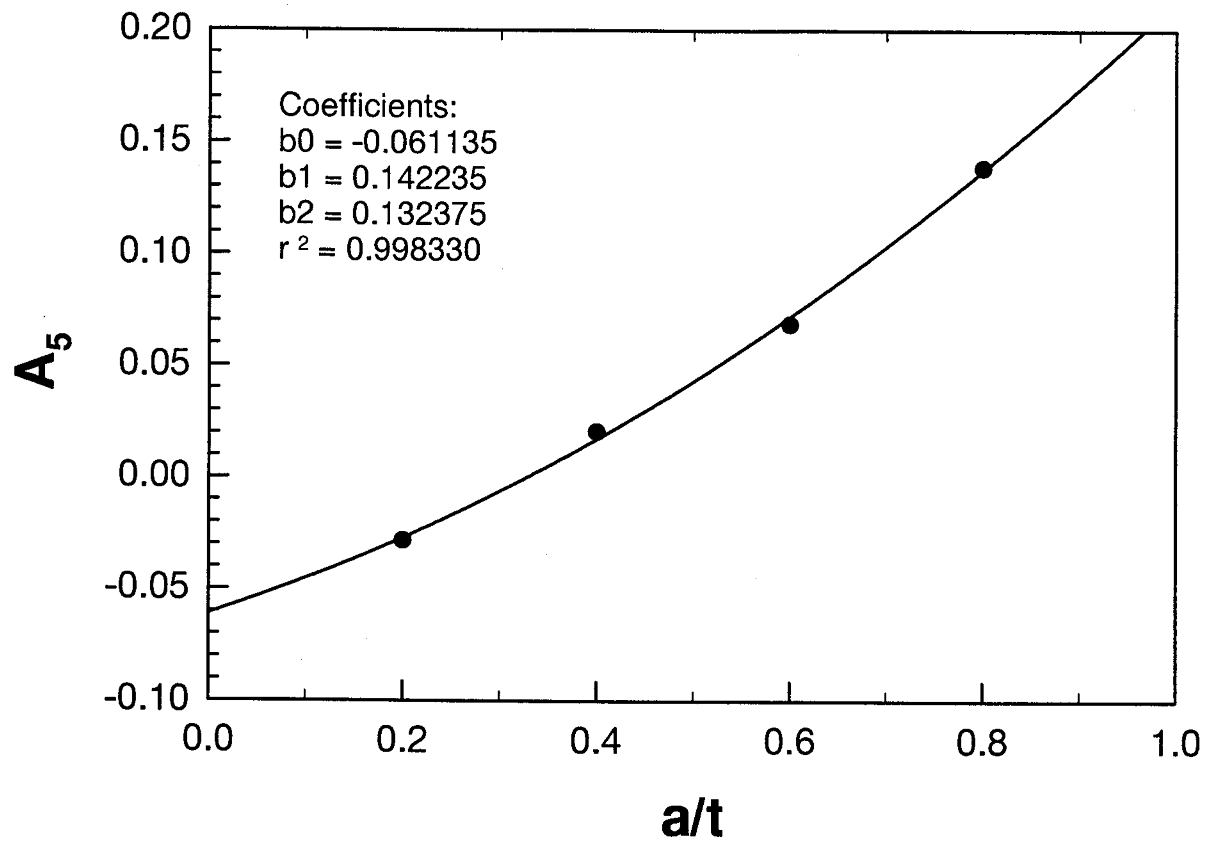

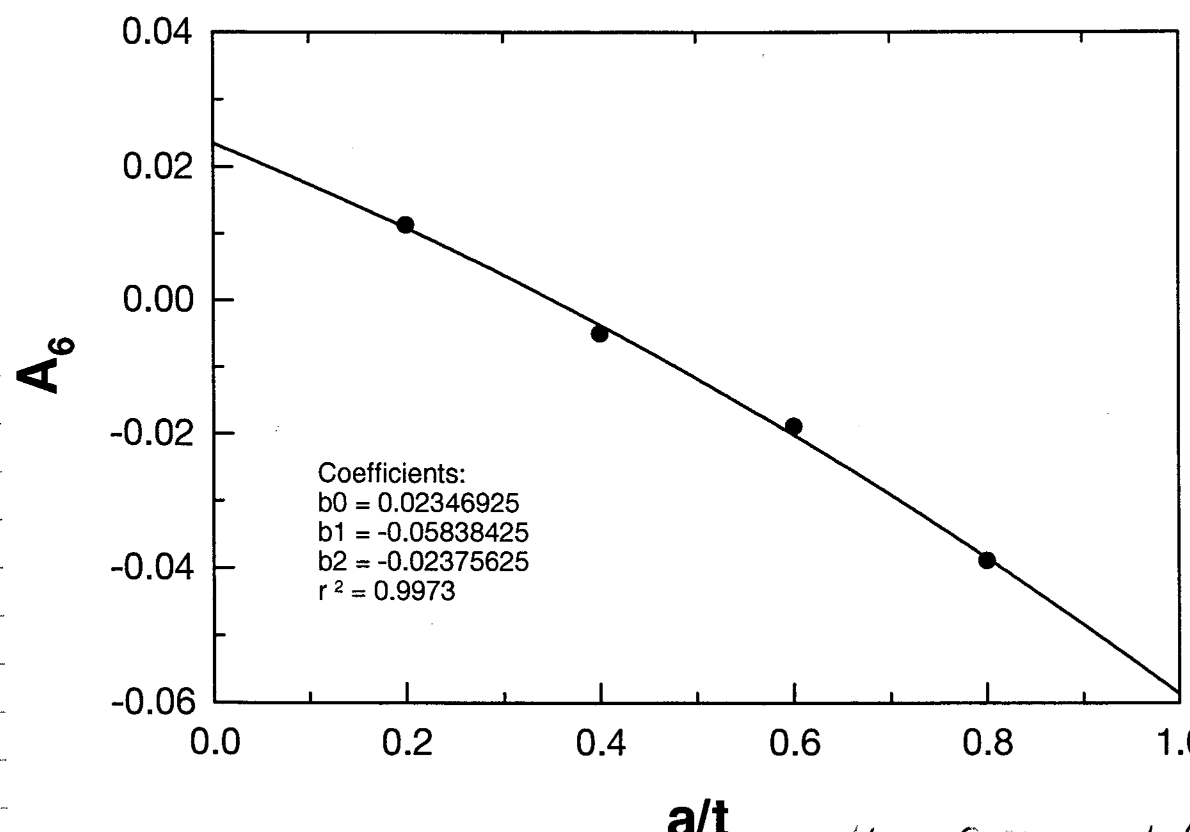

Kuai S. Chan 3/26/99

4/9/99

Collected information on the fracture toughness of Zirconium [K.C. 4/9/99] and Zircaloy-4 cladding as a function of hydrogen content.

This information was found in a paper entitled "Embrittlement of Reactor Core Materials," by P.H. Kreyns, W.F. Bourgeois, C.J. White, P.L. Charpentier, B.F. Kammenzind, and D.G. Franklin. This paper appeared in the Proceedings of the Eleventh International Symposium on Zirconium in the Nuclear Industry, ASTM STP 1295. E.R. Bradley and G.P. Sabol, eds. American Society for Testing and Materials, Philadelphia, PA, 1996, pp. 758 – 782.

Additional information on the fracture toughness of ~~Zircaloy-4 and~~ Zirconium [K.C. 4/9/99] was found in a paper by Simpson and ~~Cann~~ Cann. This paper is entitled "Fracture Toughness of Zirconium hydride and its influence on the crack resistance of zirconium alloys," Journal of Nuclear Materials, 1979, ~~pp~~ [K.C. 4/9/99] vol. 87, pp. 303 – 316.

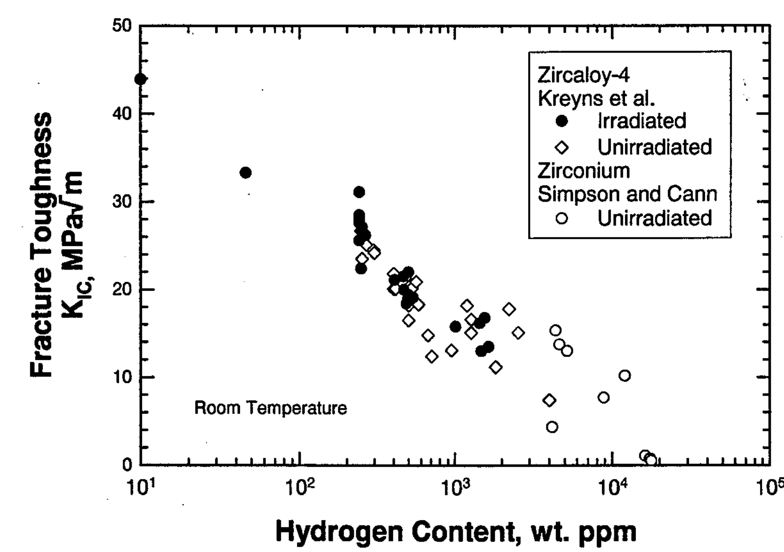

4/9/99 Kuai S. Chan

4/12/99

Performed regression analysis and fitted K_{IC} to hydrogen content.

$$K_{IC}\,(MPa\sqrt{m}) = 57.78 - 13.7 \log C_H\,(wppm) \qquad (20)$$

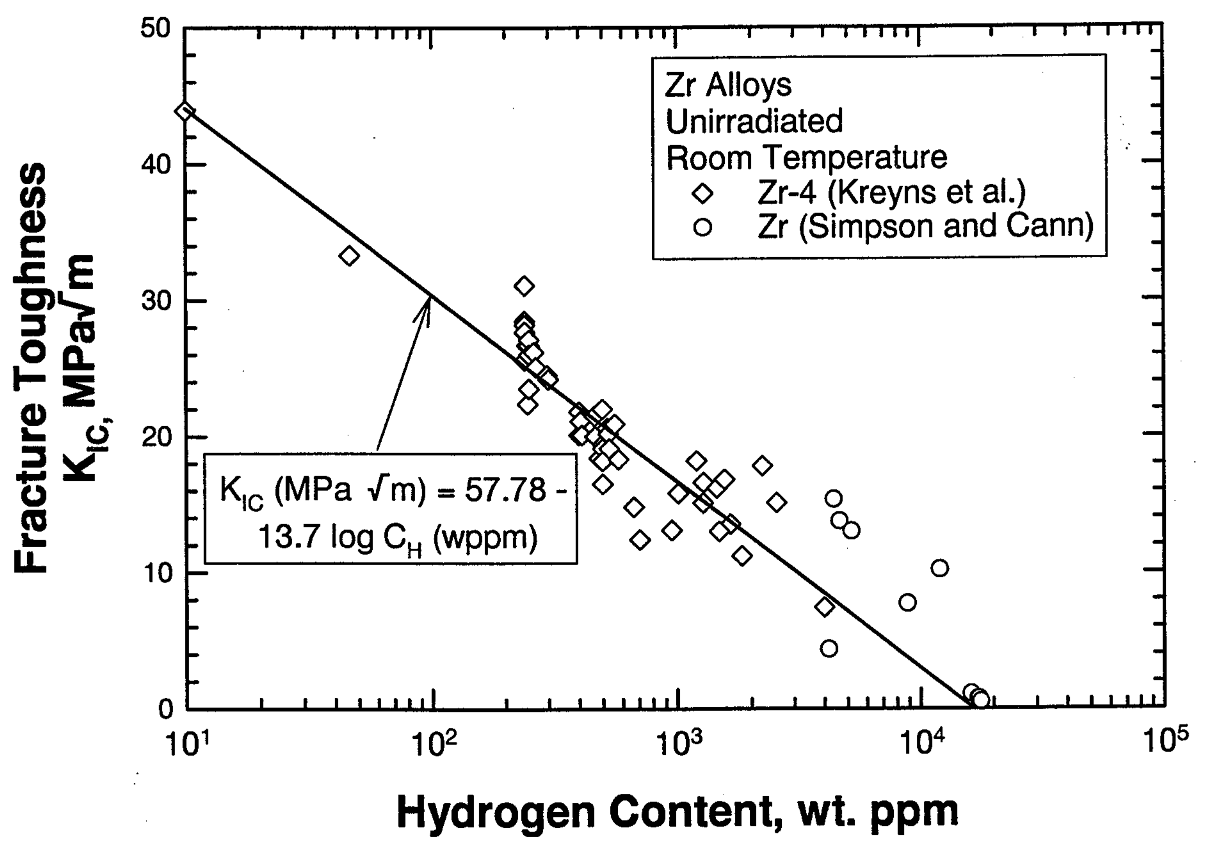

Regression analysis was performed using Sigmaplot 4.0 software.

4/12/99 Kwai S. Chan

4/22/99

Reviewed literature data of ultimate tensile strength of Zr as a function of hydrogen content.

Zircaloy-2 data was found in a paper by Marshall and Louthan, Jr. (R.P. Marshall and M.R. Louthan, Jr., Transactions of ASM, 1963, vol. 56, pp. 693-700.

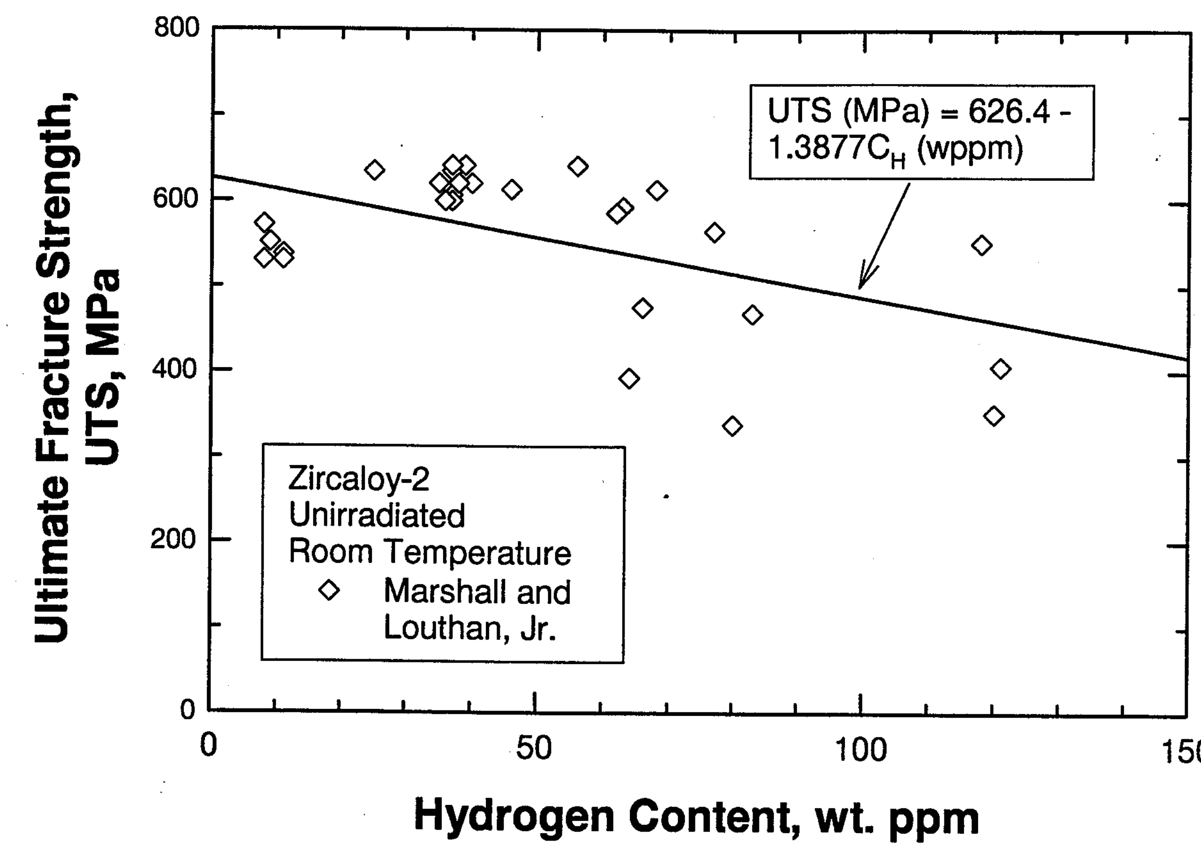

$$\sigma_{UTS} = UTS\,(MPa) = 626.4 - 1.3877\, C_H\,(wppm) \qquad (21)$$

Regression analysis was performed with Sigmaplot 4.0 software

Kwai S. Chan 4/22/99

4/26/99

UTS data for Zircaloy-4 was found ~~in~~ in a paper by Lin et al. (S.-C. Lin, M. ~~M~~ Hamasaki, and Y.-D. Chuang, Nuclear Science and Engineering, 1979, vol. 71, pp. 251 - 266.) K.C. 4/26/99

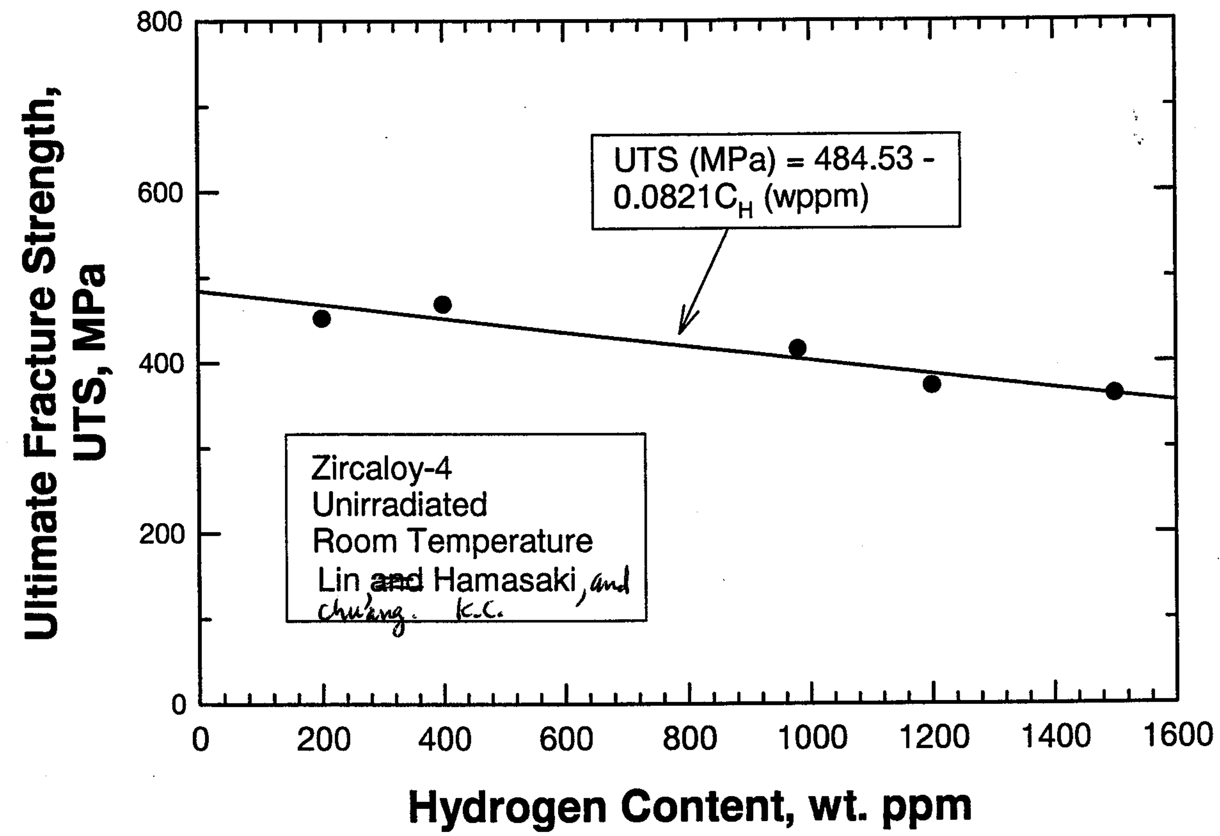

σ_{UTS} = UTS (MPa) = 484.53 − 0.0821 C_H (wppm) (22)

Regression analysis was performed ~~tak~~ using Sigmaplot 4.0 software. K.C. 4/26/99

Kwai S. Chan 4/26/99

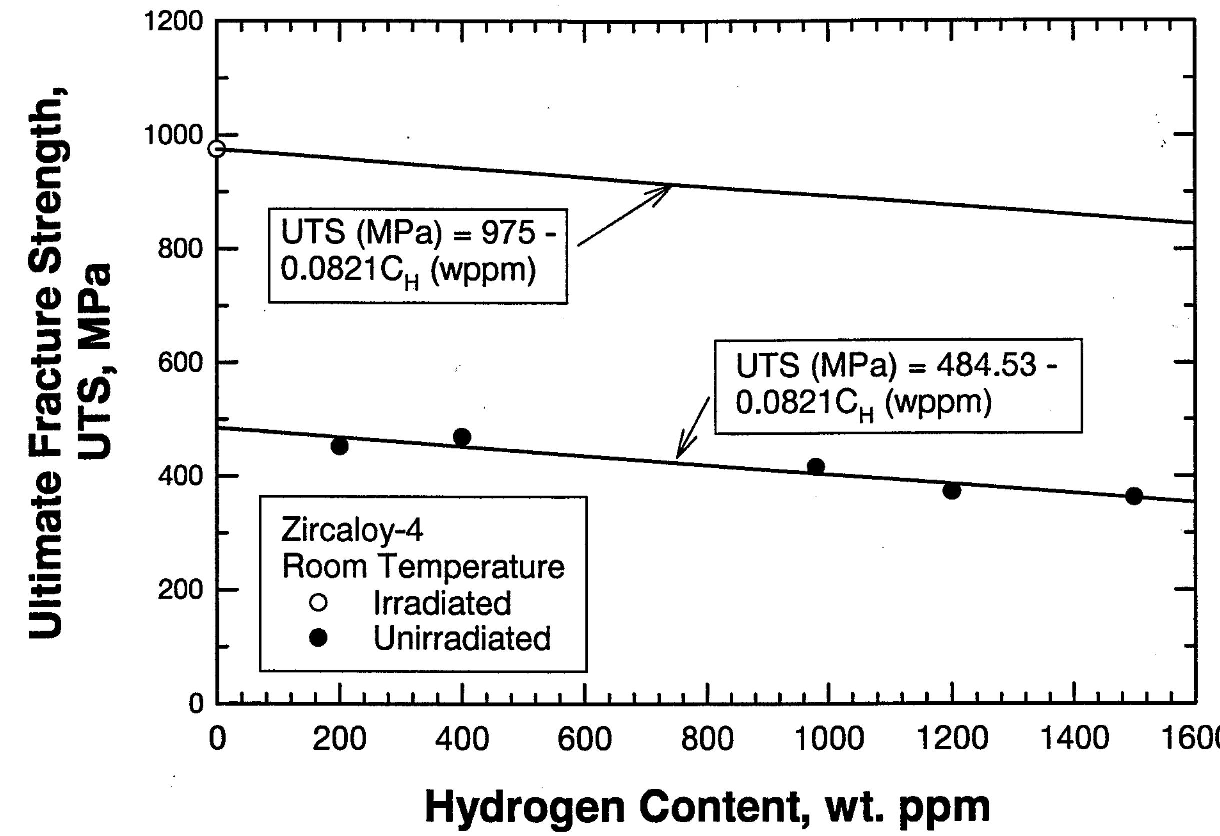

UTS of irradiated Zr-4 was constructed by using the UTS of ~~un~~irradiated Zr-4 and the slope of unirradiated Zr-4. K.C. 4/26/99

(23)

σ_{UTS} (MPa) = 975 − 0.0821 C_H (wppm) ~~for~~ K.C. 4/26/99

for irradiated Zr-4 cladding

Kwai S. Chan 4/26/99

5/7/99

Fracture Modeling of Hydrided Zr Cladding -

Assumption:

$$K_I = f_i \sigma_i \sqrt{\pi(a+a_0)} \quad (24)$$

Where K_I is the mode I stress intensity factor of a surface crack in a hydrided Zr cladding

σ_i is the stress acting on the surface crack

f_i is the geometry-correction factor

a is the ~~half-length~~ crack depth (K.C. 5/7/99) of the surface crack

a_0 is the small-crack parameter

Based on the results developed in March 2-26, 1999,

$$f_i = A_0 + A_1\left(\frac{2\phi}{\pi}\right) + A_2\left(\frac{2\phi}{\pi}\right)^2 + A_3\left(\frac{2\phi}{\pi}\right)^3 + A_4\left(\frac{2\phi}{\pi}\right)^4 + A_5\left(\frac{2\phi}{\pi}\right)^5 + A_6\left(\frac{2\phi}{\pi}\right)^6$$

(see eq. (18) on page 30). KC

Kwai S. Chan 5/7/99

For hydrided Zr cladding

$$K_{IC}\,(MPa\sqrt{m}) = 57.78 - 13.7 \log C_H\,(wppm)$$

K.C. 5/7/99 (from Eq. 20) on page 40

where C_H is hydrogen content in wt. ppm.

$$\sigma_{UTS}\,(MPa) = 975 - 0.0821\,C_H\,(wppm) \quad \text{(see Eq. 23 on P. 43)}.$$

K.C. K.C.

The value of the small-crack parameter, a_0, is evaluated by taking $a_0 \to 0$ so that $K_I = K_{IC}$ and $\sigma_i = \sigma_{UTS}$. Substituting these values of K_I and σ_i into Eq (24) leads one to

$$K_{IC} = f_0\, \sigma_{UTS} \sqrt{\pi a_0} \quad (25).$$

with $f_0 = 0.661525$ based on Eq (18) and Eq (19) using $a = 0$. (see Figure on Page 31, $a/t \to 0$) K.C. 5/7/99

Eq. 25 leads to

$$a_0 = \frac{1}{\pi}\left[\frac{K_{IC}(C_H)}{f_0\, \sigma_{UTS}(C_H)}\right]^2 \quad (26)$$

Kwai S. Chan 5/7/99

where $K_{IC}(C_H)$ and $\sigma_{UTS}(C_H)$ indicate K_{IC} and σ_{UTS} of Zr cladding ~~as~~ K.C. 5/7/99 are functions of the hydrogen content, C_H.

The critical stress for fracture of hydrided Zr cladding can be obtained by combining Eqs (24) and (26) to give

$$\sigma_{cr}(C_H) = \frac{K_{IC}(C_H)}{f_i\sqrt{\pi(a+a_o(C_H))}} \qquad (27).$$

with $a_o(C_H) = \frac{1}{\pi}\left[\frac{K_{IC}(C_H)}{f_o\,\sigma_{UTS}(C_H)}\right]^2$

Kwai S. Chan 5/7/99

5/12/99

Critical failure stress, σ_{cr}, of Zr cladding was calculation as a function of crack depth, a, for various hydrogen contents.

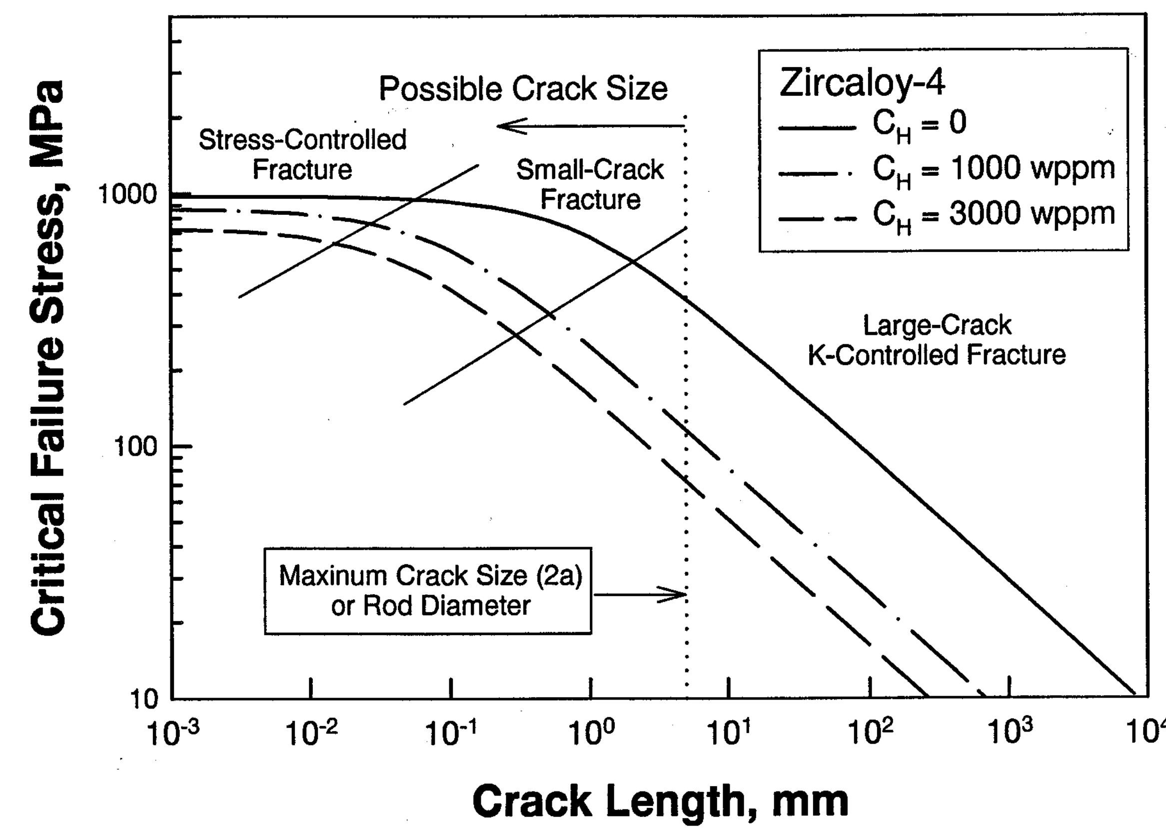

Kwai S. Chan 5/12/99

6/7/99

Developed an approach and a flow chart for the rock fall model.

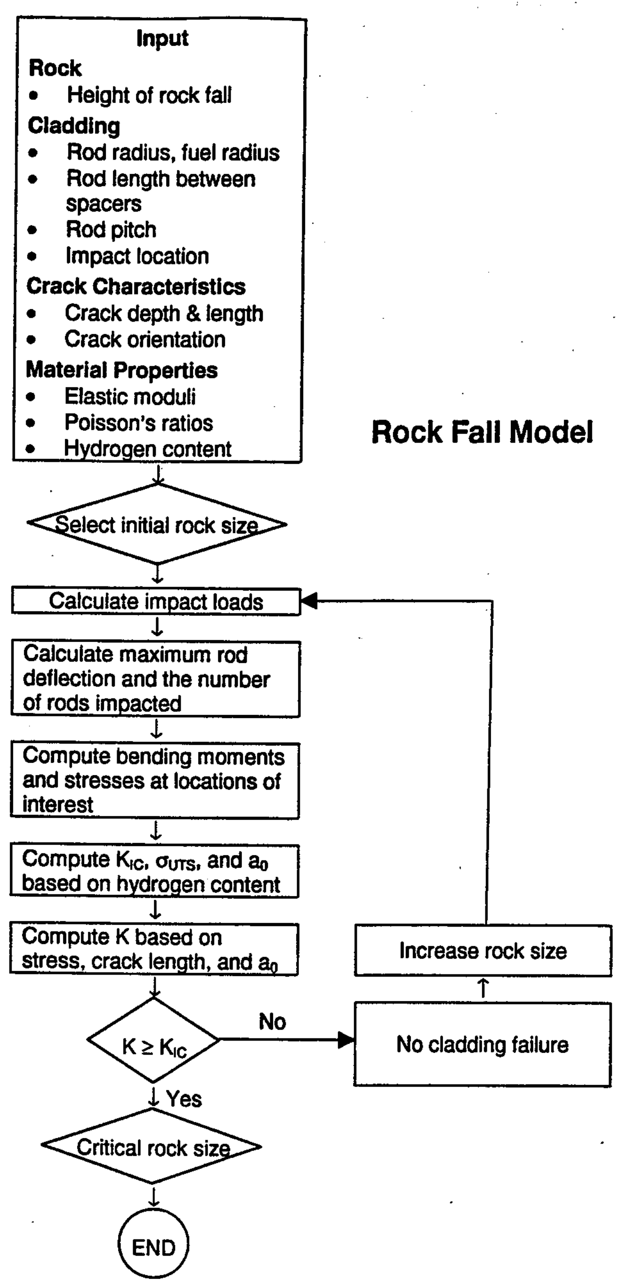

Kwai S. Chan 6/7/99

Oct 20, 2000

Work Description: Reviewed DOE approach for treating hydride-~~delayed~~ related (K.C. 10/20/2000) degradation of SNF cladding under Repository Conditions

Document Reviewed: ANL-EBS-MD-000011 REV 00

"Hydride-Related Degradation of SNF Cladding Under Repository Conditions."

Nov 10, 2000

~~Nov 10, 2000~~ K.C. 11/10/2000

Work Description: Review of DOE's approach on hydride-related degradation of SNF cladding continued.

Nov 22, 2000

~~Nov 22, 2000~~ K.C. 11/22/00

Work Description: Reviewed DOE document on initial cladding conditions

Document reviewed: ANL-EBS-MD-000048, Rev. 00A

ANL-EBS-MD-00045, Rev 00

Kwai S. Chan 11/22/99

Nov 27, 2000

Work Description: Continued to review DOE document on Initial Cladding Conditions

Calculated cladding stresses at 260°C Based on DOE results on crack depth and K_I values for 260°C (CRWMS, 2000, pp. 31, 33, 34, 46, 47)

The cladding stress at 260°C were computed based on the crack depth and the K_I values for 260°C using the DOE K_I expression (CRWMS M&O, 2000a, Eq. 6.10-2, p. 46).

	Crack Depth, μm	Cladding Stress, MPa (at 27°C)	K_I, MPa$\sqrt{m}$ (260°C)	Cladding Stress, MPa (260°C)
median	13.0	35.8	0.40	62.6
mean	18.6	38	0.47	61.5
5%	54.5	61.8	1.078	82.4
maximum	119	146	2.7	139.6

The threshold stress for hydride reorientation is ≈ 69 MPa. Thus, the cladding stress at 260°C is sufficiently high for hydride reorientation to occur.

Kwai S. Chan
11/29/00

Nov 28, 2000

Work Description: Review DOE documents on Clad degradation and modeling approach

Document Reviewed: ANL-WIS-MD-000008 REV00

"Clad Degradation - FEPs Screening Arguments"

TDR-WIS-MD-000001 REV 00

"Waste Form Degradation Process Model Report"

Preparation of reviews for inclusion into IRSR ~~report~~ K.C. K.C. 11/28/00 started.

Nov 29, 2000

~~Nov 29, 2000~~ K.C. 11/29/00

Work Description: continued to work on report

First draft completed.

Nov 30, 2000

~~Nov 30, 2000~~ K.C. 11/30/00

Work Description: attended Report Status Meeting

Revised Report.

Kwai S. Chan
11/30/00

Dec 1, 2000

Work Description: Revised and completed report

Report submitted.

K.C. 3/29/01

~~March 27, 2001~~

March 27, 2001

Work Description: Revied Report entitled "Breakage of Commercial Spent Nuclear Fuel Cladding by Mechanical Loading," by Kevin McCoy.

Ref: CAL-EBS-MD-000001 REV 00

K.C. 3/29/01 March 28, 2001 K.C. 3/29/01

~~March 28, 2001~~

Work Description: continued to review the report. Started writing the review.

March 29, 2001 K.C.

~~March 29, 2001~~ 3/29/01

Work Description: completed and submitted the review.

Kwai S. Chan
3/29/01

Review of "Breakage of Commercial Spent Nuclear Fuel Cladding by Mechanical Loading," Document CAL-EBS-MD-000001 REV 00, by J. K. McCoy, 1999.

This report documents the results of analytical calculations performed to assess the failure rates of commercial spent nuclear fuel cladding (CSNF) by mechanical loading during storage in a waste repository. The calculation methods, assumptions, input parameters, and computational results are described in detail in the report.

Two sources of mechanical loads were considered in the risk assessment calculations, which included seismic loading and impact loading by rock fall. The failure modes considered for CSNF rods were rupture and fracture. The approach taken was to compute the stresses in the cladding rods due to seismic loading or impact loading by rock fall. The probabilities of rod failure by rupture and fracture were computed for a given impact velocity, which was in turn related to the peak ground acceleration of an earthquake at a particular strength. The total failure rate was then computed by summing the contributions by earthquakes of all strengths. This approach appeared to be reasonable.

The rupture criterion was formulated in terms of the yield stress, while the fracture criterion was based on linear-elastic fracture mechanics and the fracture toughness for irradiated rods. A rupture criterion based on the onset of yielding is reasonable and conservative for irradiated rods. Hollow rods were assumed in the computation of the cladding stress. This is likely to give higher cladding stresses and therefore conservative results. The effect of loading rate on the yield stress was not considered in the analyses, but it probably did not introduce significant errors to the results. The distribution of yield strengths was not considered. This omission could alter the failure rate significantly, and it should be addressed.

An exponential flaw distribution was assumed in the calculation of the failure probability for fracture. The assumed flaw distribution was reasonable. However, it is uncertain that the flaw distribution would give conservative estimates. The low failure probability computed for fracture by seismic loading was probably the consequence of small crack sizes in the cladding and the use of a fracture criterion based on large-crack fracture mechanics. Since failure that involved small cracks would be captured by the rupture criterion, the total failure rates probably were not significantly affected and the large-crack formulation appeared to be reasonable. On the other hand, the author's argument that the risk to fracture would be small regardless of the fracture properties, the number of flaws, and the flaw size distribution was not supported by any calculations. A systematic evaluation of these variables through the appropriate parametric calculations are needed to support this claim.

The use of a point load to represent impact loading by rock fall was justified, since pervious work (Chan and Lee, Nuclear Engineering and Design, vol. 201, 2000, pp. 209-226) showed that a point load formulation would give the same result as a distributed load formulation. The placement of the point load at the critical location (one-third of the rod length) was also justified based on the prior work. The critical point corresponds to the impact location that induces the maximum bending moment and stress at one of the fixed ends. Thus, it represents the worst case. The conclusion that all rods would fail by rock fall is also supported by results in the literature (Chan and Lee, 2000).

Kwai S. Chan 3/29/01

April 10, 2001

Work Description: Reviewed Initial Cladding Condition

Ref: ANL-EBS-MD-000048 REV 00 ICN 01

April 11, 2001 4/11/01
~~April 11, 2001~~ K.C.

Work Description: Reviewed Clad Degradation — FEPs Screening Arguments

Ref: ANL-WIS-MD-000008 REV 00 ICN 01

April 12, 2001 4/13/01
~~April 12, 2001~~ K.C.

Work Description: Reviewed Thermal History of Cladding in a 21 PWR SNF WP Loaded With Average Fuel

Ref: CAL-UDC-ME-000001 Rev 00

April 13, 2001 4/13/01
~~April 13, 2001~~ K.C.

Work Description: Reviewed Hydride-Related Degradation of SNF Cladding Under Repository Conditions

Ref: ANL-EBS-MD-000011 Rev 00.

Kwai S. Chan
4/13/01

April 16, 2001

Work Description: Reviewed Clad Degradation — Summary and Abstraction

Ref: ANL-WIS-MD-000007 REV 00

April 17, 2001 4/17/01 K.C.
~~April 17, 2001~~

Work Description: Completed and submitted Review

DOE's arguments are not consistent with cladding temperatures and stresses documented in Clad Degradation -Summary and Abstraction (CRWMS M&O, 2000f, p.19 and 20). According the DOE's analyses, the center rod in an average WP will reach 308°C and the outer rods will peak at 291°C. The temperature uncertainty is uniformly distributed over a range of ± 13.5% Thus, the hottest center rod in an average WP will peak at 350° C while the hottest outer rod will peak at 314°C. The solubility of hydrogen in Zircaloy are 80 and 120 ppm at 314°C and 350°C, respectively (CRWMS, M&O, 2000e, p. 57). The average hydrogen content in commercial spend fuel rods is about 400 ppm in the form hydrides. At the fuel rod temperature increases to the peak temperature, some of the hydrides would dissolve and go back into solution. The dissolved hydrogen will re-precipitate as radial hydrides, if the cladding stress exceeds a critical value during the precipitation process. The tensile stress for hydride reorientation is between 69 to 208 MPa. (CRWMS M&O, 2000h) DOE's calculation of the cladding stresses over the temperature range of 250° - 385°C are between 55 MPa and 120 MPa. This range of stresses is well within the minimum tensile stress for hydride reorientation to occur when the cladding cool slowly below the solvus temperature in the repository.
.

After an evaluation of six creep models against five set of experimental data, DOE elected Murty's creep model over other five models including the one by Matsuo. DOE claimed that Murty's creep equations are accurate at low stresses and low temperatures because it incorporates Coble creep, which is dominant at low stresses and low temperatures. In addition to Coble creep, Murty' creep equations include primary and steady-state creep by dislocation glide, the same creep mechanisms treated in Matsuo's model. Model uncertainty in creep correlations of all five set of experimental data is 0.487 for Matsuo's model and it is 0.557 for Murty's model. A critical strain criterion was used for creep failure. Upper and lower limits of rod failure by creep were computed based on creep failure strain limits of 0.4% and 11.7%. These creep failure strains were supported by experimental data of unirradiated Zircaloy and corresponded to an average creep failure strain of 3.3% used in an earlier analysis concerning cladding failure by creep during dry storage and transportation (CRWMS M&O, 2000d). The Murty's model and the creep strain criteria are acceptable since they both lead to conservative failure estimates.

Kwai S. Chan
4/17/01

I have reviewed this scientific notebook and find it in compliance with QAP-001. There is sufficient information regarding procedures used for conducting tests, acquiring and analyzing data so that another qualified individual could repeat the activity.

6/28/02

VIJAY JAIN